Edward L. Ginzton Laboratory of Physics
Stanford University
Stanford, California 94305

Final Technical Report
February 1, 1982 to December 31, 1985

N.A.S.A. Grant NAG 5-220

GROWTH AND EVALUATION OF $AgGaS_2$ and $AgGaSe_2$ FOR INFRARED NONLINEAR APPLICATIONS

Principal Investigators

Robert L. Byer
Applied Physics Department

and

Robert S. Feigelson
Center for Materials Research

Ginzton Laboratory Report No. 3994

February, 1986

GROWTH AND EVALUATION OF $AgGaS_2$ and $AgGaSe_2$ FOR INFRARED NONLINEAR APPLICATIONS

Robert L. Byer
Applied Physics Department
Stanford University, Stanford, CA 94305

and

Robert S. Feigelson
Center for Materials Research
Stanford University, Stanford, CA 94305

ABSTRACT

Significant advances have been made in the growth technology of silver thiogallate ($AgGaS_2$) and silver selenogallate ($AgGaSe_2$) in this program. We have demonstrated high efficiency harmonic generation of carbon dioxide laser radiation and tunable infrared parametric oscillation using these materials. Nonlinear frequency conversion in the infrared has been limited by the optical properties and the size of the available nonlinear materials. The development of these materials has reduced some of the limitations and generated wide interest. The continued development and application $AgGaS_2$ and $AgGaSe_2$ now appears assured.

Table of Contents

Personnel Associated with the Program

Robert L. Byer
Professor, Applied Physics Department

Robert S. Feigelson
Professor, Center for Materials Research

Roger K. Route
Senior Research Associate, Center for Materials Research

Robert C. Eckardt
Senior Research Associate, Ginzton Laboratory

Yuan Xuan Fan
Visiting Scholar, from Shangai Institute of Laser Technology

Gregory Magel
Research Assistant -Graduate Student

Thomas Kane
Research Assistant -Graduate Student

GROWTH AND EVALUATION OF $AgGaS_2$ and $AgGaSe_2$ FOR INFRARED NONLINEAR APPLICATIONS

Robert L. Byer and Robert S. Feigelson

A. SUMMARY OF RESEARCH RESULTS.

The objective of this program was to improve the crystal growth technology for the two chalcopyrite materials silver thiogallate ($AgGaS_2$) and silver selenogallate ($AgGaSe_2$) and to demonstrate the use of these materials for nonlinear infrared frequency conversion. The potential of these materials for this application was demonstrated in the early 1970's. However, a number of serious growth related problems had to be solved to permit the growth of high optical quality and larger size material required for nonlinear frequency conversion. Other potential nonlinear infrared materials have had similar problems, and the quality of available nonlinear materials of adequate size has limited progress in nonlinear frequency conversion at infrared wavelengths. $AgGaS_2$ and $AgGaSe_2$ are the first nonlinear infrared materials developed to the extent that they should find wide-spread use for nonlinear infrared frequency conversion.

The growth-related problems of these two materials are similar, and experience first gained with the thiogallate was directly applicable to the selenogallate. Both are volatile at their melting temperatures and must be grown in sealed ampoules using the Bridgman-Stockbarger technique. Both have anomalous expansion along the c axis. Therefore, it is necessary to seed the growth in the c-direction and to use precision-tapered ampoules to avoid cracking when cooling after growth. Large crystals solidify only with non-stoichiometric composition resulting in finely dispersed scattering centers and reduced infrared transmission in the as-grown materials. Post-growth heat treatment is required to remove the scattering and provide high optical quality. Boules of 2.8 cm diameter by 10 cm length have been successfully grown and heat treated for each material. The growth technology of $AgGaS_2$ has been transferred to industry, and that material is now available commercially. The boule size of $AgGaSe_2$ is now being increased to 4-cm diameter. Further discussion of the growth technology is given in Appendix A.

Much interest has resulted from our preliminary demonstrations of nonlinear infrared frequency conversion with these chalcopyrite materials. We have reported tunable infrared parametric oscillation in $AgGaS_2$ and high-efficiency second harmonic generation of carbon dioxide laser radiation in $AgGaSe_2$. A brief history and current status of nonlinear infrared materials is contained in Appendix B. Infrared parametric oscillation in $AgGaS_2$ is described in Appendix C, and second harmonic generation of 10-μm radiation in Appendix D. Only a brief summary of these results is presented in this summary. We have also recently observed infrared parametric oscillation in $AgGaSe_2$, however, these results are not yet published.

$AgGaS_2$ is transmitting between 0.45 and 13 μm with some multiphonon absorption at wavelengths longer than 9 μm. The transparency range in $AgGaSe_2$ extends from 0.73 to 17 μm with multiphonon absorption shifted to wavelengths longer than 13 μm. The phasematching range in the selenogallate is also shifted to longer wavelengths. For example angle tuned type I second harmonic generation is possible in $AgGaS_2$ for fundamental wavelengths between 1.8 to 11 μm whereas the corresponding range for $AgGaSe_2$ is 3.1 - 13 μm. The two materials are complementary in the sense that one has better characteristics at longer wavelengths while the other permits processes at shorter wavelengths. $AgGaS_2$ is useful for mixing processes that involve visible or near-infrared wavelengths. For example, that material can be used for upconversion to the visible and parametric oscillation pumped by 1.06-μm neodymium lasers, but phasematching for these processes is not possible in $AgGaSe_2$. However, the selenogallate is superior for harmonic generation of 10-μm CO_2 radiation and for parametric oscillation pumped by wavelengths between 1.6 and 7 μm. The nonlinear optical coefficient is $d_{36} = 43 \times 10^{-12}$ m/V for the selenogallate, and it is $d_{36} = 18 \times 10^{-12}$ m/V for the thiogallate. Both materials have been fabricated with absorption coefficients as low as 0.02 cm^{-1}. And both materials have surface damage thresholds of 13 MW/cm^2 for 20 nsec duration infrared pulses.

Infrared parametric oscillation was demonstrated in $AgGaS_2$ with output continuously adjustable from 1.4 - 4.0 μm by angle tuning of the crystal. The pump source for this experiment was a 1.064-μm, Q-switched Nd:YAG laser with a 20-ns duration output pulse. The transverse distribution was Gaussian-like with a beam waist of 0.7 mm. Threshold for parametric oscillation was 1.5 mJ. Energy conversion efficiency of 16% was reached near degeneracy where the output wavelength is 2.13 μm. Our nonlinear frequency conversion demonstrations have been of a preliminary nature with performance characteristics that could easily be improved with optimization of experimental conditions. The infrared parametric oscillator performance would improve with the use of a pump beam with larger and flatter transverse distribution. Also, any improvement in the

nonlinear material such as decreased losses, higher damage threshold or longer interaction length will be reflected in improved parametric oscillator performance. With such improvements the tuning range of these parametric oscillators could be extended to the transparency limit of the material, 13 μm.

Harmonic generation of CO_2 laser radiation has not been widely used because of the limitations of available nonlinear infrared materials. $AgGaSe_2$ is well suited for this application, and our initial demonstration of its use has generated much interest. We have demonstrated 14% internal energy conversion efficiency using a 2-cm crystal of $AgGaSe_2$. The pump pulse, generated by a pulsed TEA laser, had a 75-ns gain-switched spike followed by a 650-ns nitrogen tail. Power conversion efficiency at the peak of the spike was calculated to be 60%. This measurement was performed with an uncoated crystal which had 20% reflection losses at each surface. We have found that it is possible to increase damage threshold from 13 MW/cm^2 to 37 MW/cm^2 with the application of antireflection coatings. This increase in damage threshold will permit an increase in fundamental intensity that will significantly improve harmonic conversion efficiency. $AgGaSe_2$ is also useful for generating other harmonics of the CO_2 laser and for infrared parametric oscillation.

We have achieved parametric oscillation in $AgGaSe_2$ using two different pump sources. Output tuning over the range of 1.6 - 1.7 μm and 6.7 - 6.9 μm was obtained using a 1.34-μm Nd:YAG laser, and continuous tuning was obtained between 3.3 and 5.6 μm using a 2.05-μm Ho:YLF laser in a collaborative experiment with the Naval Research Laboratory. Angle-tuned, 2-cm crystals were used in these measurements. Both lasers provided linearly polarized Q-switched pulses with Gaussian-like transverse intensity distributions. The crystal used in the Nd:YAG-pumped oscillator was tuned over the 77^o - 90^o range. Both end surfaces were antireflection coated with ThF_4. Conversion efficiency of 18% was obtained with the Nd:YAG pump with output tuned to 1.66 μm. Parametric oscillation was obtained with both antireflection coated and uncoated crystals in the Ho:YLF pumped oscillator. The antireflection coated crystal had 30% internal losses whereas the uncoated crystal had 40% surface reflection losses but only 2% internal losses.

The point again is that these are preliminary demonstrations. The heat treatment of $AgGaSe_2$ remains an active topic of research. The fact that parametric oscillation could be achieved with a 2-cm crystal with 30% internal losses or an uncoated crystal is encouraging. The high-quality crystal is now being antireflection coated, and further experiments are planned for March of 1896.

We are also considering other schemes such as using a 1.06-μm pumped parametric oscillator for difference frequency generation in $AgGaSe_2$. With this two-step system, the infrared radiation generated would be continuously tunable from 1.3 to 17 μm. Another possibility is to use the third or fourth harmonic of CO_2 laser radiation for the pump.

The further development of the chalcopyrite materials $AgGaS_2$ and $AgGaSe_2$ has provided valuable and much-needed nonlinear infrared materials. Support for continued research in the growth and application of the materials has been provided by the U. S. Army Research Office and the Office of Naval Research. Extending the growth to larger crystal sizes, improving quality by development of the heat treatment process, and the development of processing techniques for reducing surface damage thresholds remain active areas of research. Work on extending frequency conversion ranges, improving conversion efficiency, and in general gaining better control of the properties of nonlinear frequency conversion processes also remains active.

B. PUBLICATIONS AND PRESENTATIONS.

PUBLICATIONS.

1. R.L. Byer and Y.X. Fan, "Progress in Optical Parametric Oscillators," SPIE Proc., vol. 461, New Lasers for Analytical and Industrial Chemistry, p. 27, 1984.

2. Y.X. Fan, R.C. Eckardt, R.L. Byer, R.K. Route and R.S. Feigelson, "$AgGaS_2$ Infrared Parametric Oscillator," Appl. Phys. Lett., vol. 45, pp. 313-315, Aug. 15, 1984.

3. R.C. Eckardt, Y.X. Fan, R.L. Byer, R.K. Route, R.S. Feigelson, and Jan van der Laan, "Efficient Second Harmonic Generation of 10-Micron Radiation in $AgGaSe_2$," Appl. Phys. Lett., vol. 47, pp. 786-788, Oct. 15, 1985.

4. R.S. Feigelson and R.K. Route, "Recent Developments in the Growth of Chalcopyrite Crystals for Nonlinear Infrared Applications," to be published, SPIE Proc.

PRESENTATIONS.

1. Y.X. Fan and R L. Byer, "An Infrared $AgGaS_2$ Optical Parametric Oscillator," post-deadline paper Conference on Lasers and Electro-Optics, Baltimore, MD, May 1983.

2. R.L. Byer, "Efficient Nonlinear Conversion of Laser Sources in Crystals," NASA Workshop on Tunable Solid State Lasers for Remote Sensing, Menlo Park, CA. Oct. 1984.

3. R. Eckardt, "Infrared Frequency Conversion in Chalcopyrite Crystals: $AgGaS_2$ and $AgGaSe_2$," NASA Workshop on Tunable Solid State Lasers for Remote Sensing, Menlo Park, California. Oct. 1984.

4. R.C. Eckardt, Y.X, Fan, R.L. Byer, R.K. Route and R.S. Feigelson, "Efficient, Practical Second Harmonic Generation of 10.6 microns in $AgGaSe_2$," paper ThM28, The Conference on Lasers and Electro-Optics, Baltimore, May 1985.

5. R.S. Feigelson, R.K. Route, R.L. Byer, R.C. Eckardt and Y.X. Fan, "Recent Developments in Chalcopyrite Crystals for Nonlinear Infrared Applications", Paper 567-O2, SPIE's 29th Annual International Technical Symposium on Optical and Electro-Optical Engineering, San Diego, August 1985.

Efficient second harmonic generation of 10-μm radiation in $AgGaSe_2$

R. C. Eckardt, Y. X. Fan, and R. L. Byer
Applied Physics Department, Stanford University, Stanford, California 94305

R. K. Route and R. S. Feigelson
Center for Materials Research, Stanford University, Stanford, California 94305

Jan van der Laan
SRI International, Menlo Park, California 94025

(Received 17 June 1985; accepted for publication 29 July 1985)

$AgGaSe_2$ crystals for nonlinear infrared applications are being grown reproducibly. Using high-quality, 2-cm-long crystals, 14% energy and 60% peak intensity conversion efficiency have been demonstrated for second harmonic generation of the pulsed output of a CO_2 miniature transversely excited atmospheric laser.

The use of silver gallium selenide for nonlinear infrared applications was proposed in 1972.[1] Further characterization and initial demonstrations of second harmonic and difference frequency generation in this material soon followed.[2,3] However, at the time, growth-related problems made it difficult to obtain high-quality crystals of adequate size. Other potential nonlinear infrared materials had similar problems, and the lack of high-quality nonlinear materials of adequate size has limited progress in nonlinear frequency conversion for infrared wavelengths.

We are now growing 2.8-cm-diam boules of $AgGaSe_2$, each of which yields several high-optical quality nonlinear crystals of 2 cm length. The use of $AgGaSe_2$ for second harmonic generation (SHG) of a CO_2 pulsed laser output with 14% harmonic energy conversion efficiency is reported in this letter. This is an initial demonstration with this new material, and other nonlinear applications are being investigated. It is expected that the crystal growth technology is scalable to larger sizes so that improved conversion efficiencies are possible.

A brief review of second harmonic conversion of CO_2 laser radiation illustrates some of the problems that have limited nonlinear infrared frequency conversion in the past. The highest reported second harmonic energy conversion efficiency of a CO_2 laser pulse, 27%, was obtained in $CdGeAs_2$.[4] That semiconductor material has a small band gap and must be cooled to cryogenic temperatures to reduce absorption. $CdGeAs_2$ has also been found difficult to grow, and its availability is very limited.

A number of other potential nonlinear infrared materials were proposed in the early 1970's.[5] Harmonic conversion in most of these materials was limited to less than a few percent because of problems of optical damage, small interaction length, and poor optical quality.

Tellurium has been considered for harmonic generation of the CO_2 laser, but has not gained widespread use because of its large birefringence and multiphoton absorption which have limited harmonic conversion to about 5%.[6] Tellurium has the additional problem of being difficult to fabricate.

"Stack of plates" harmonic converters allow the use of nonlinear materials that cannot be phase matched in bulk. Such devices, however, are also difficult to fabricate because the individual plates are very thin. Second harmonic power conversion efficiency of 2.7% has been demonstrated with a stack of 19 GaAs plates.[7] The thickness of each plate was limited to the coherence length which is 0.1 mm in nonbirefringent GaAs.

There is currently a renewed interest in nonlinear infrared frequency conversion due in part to recent improvements in the growth of some nonlinear materials. Specifically, $AgGaS_2$,[8] $AgGaSe_2$, and Tl_3AsSe_3 (Ref. 9) are now being grown in good quality larger single crystals. Both $AgGaSe_2$ and Tl_3AsSe_3 are useful for second harmonic generation of CO_2 laser output. $AgGaS_2$ is similar to $AsGaSe_2$ except that regions of transmission and phase matching are shifted to shorter wavelengths, and it has a lower nonlinear coefficient. $AgGaS_2$ is useful for nonlinear frequency conversion in the 0.5–10 μm wavelength range. An intrinsic three-phonon absorption of 0.6 cm^{-1} near 10 μm in $AgGaS_2$,[10] however, limits its use for second harmonic generation of CO_2.

The growth-related problems of $AgGaS_2$ and $AgGaSe_2$ are similar, and experience gained with previous growth of the sulfide was directly applicable to the growth of the selenide. Both materials are volatile at their melting temperatures and must be grown in sealed ampoules using the Bridgman–Stockbarger technique. Both also have anomalous expansion along the c axis.[11] Therefore, it is necessary to seed the boules in the c direction and to use precision-tapered ampoules to avoid cracking when cooling after growth. Large crystals can only be grown with nonstoichiometric composition which results in finely dispersed scattering centers. Post-growth heat treatment in the presence of access Ag_2Se in the case of $AgGaSe_2$ is then required to remove the scattering centers.[12] Boules of 2.8 cm diameter by 10 cm length have been successfully grown and heat treated. Each boule yields three or four good quality nonlinear crystals of 1 cm aperature by 2 cm length.

Our 2.1 cm $AgGaSe_2$ crystal had a transmission loss 7.6% in excess of that calculated for Fresnel reflections. An absorption coefficient of 0.06 cm^{-1} is indicated if there are no other losses. Further optimization of the heat treatment procedure should reduce the absorption. Coefficients as low as 0.01 cm^{-1} at 10.6 μm have been achieved in other $AgGaSe_2$ samples.

Second harmonic generation of the output of a CO_2 transversely excited atmospheric (TEA) laser was chosen to demonstrate the nonlinear performance of this material. $AgGaSe_2$ is a negative uniaxial crystal with $\bar{4}2m$ symmetry.

 0003-6951/85/200786-03$01.00

TABLE I. Some phase-matching parameters for second harmonic generation in $AgGaSe_2$ for two CO_2 wavelengths.

Wavelength	10.25 μm	5.125 μm	10.6 μm	5.30 μm
n_o	2.5934	2.6143	2.5915	2.6136
n_e	2.5603	2.5815	2.5585	2.5809
phase-matching angle θ_m	52.7°		55.0°	
angular acceptance $\delta\theta$ (for a 2 cm crystal)	0.42°		0.50°	
birefringent walkoff ρ	0.69°		0.67°	

Only type I phase matching is possible for second harmonic generation of the CO_2 wavelengths near 10 μm due to the small birefringence of the material. A list of some of the phase-matching parameters determined from Sellmeier equations for the material[2] is given in Table I. The angular acceptance angle $\Delta\theta$ is approximated by the angle between the peak and first minimum of the small single tuning curve. It is proportional to $1/l$ where l is the crystal length. Angular acceptance for the 2.1-cm crystal used for these measurements is 0.4°. This value is an internal angle; the external angular acceptance is obtained by multiplying by the index of refraction. The displacement due to the birefringent walkoff was 0.26 mm for the 2.1-cm crystal. Phase-matching parameters are tabulated at two wavelengths; 10.25 μm, the wavelength at which the measurements reported here were made, and 10.6 μm, the wavelength of the strongest CO_2 laser line.

Figure 1(a) shows a schematic of the apparatus used for SHG measurements. A grating tuned miniature TEA laser operating on the R (20) transition was used for this measurement. The laser wavelength was determined with a grating spectrometer. The laser beam was focused into the $AgGaSe_2$ crystal with a long radius-of-curvature mirror. Adjustment of the pump intensity was obtained by placing the nonlinear crystal at different positions in the focused beam. Beam size and divergence were within the limits required to permit the use of the plane wave approximation for the analysis of harmonic generation.

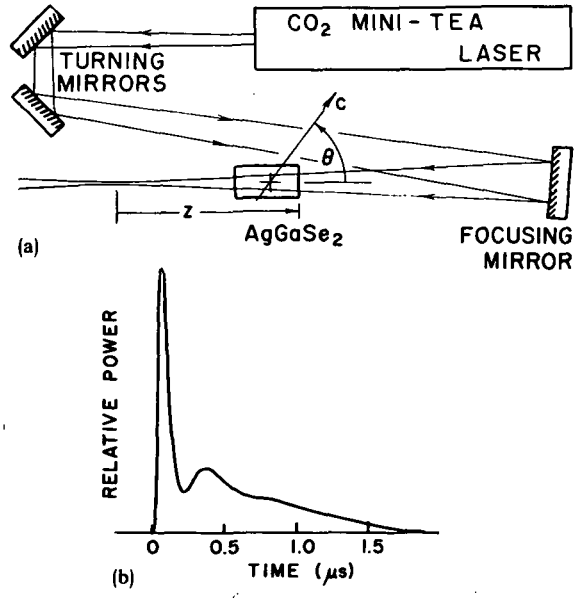

FIG. 1. (a) Schematic drawing of experimental setup used to measure second harmonic generation and optical damage threshold. (b) Temporal power distribution of the miniature TEA CO_2 laser pulse used for these measurements.

The temporal distribution of the laser pulse consisted of a gain switched spike 75 ns wide at the half-peak power points followed by a 650-ns nitrogen tail as shown in Fig. 1(b). The spike contained 35% of the total pulse power. A 1-ns rise time, room-temperature HgCdTe detector was used to observe temporal profiles. Transverse spatial profiles were measured with a slit which was scanned across the beam. A pyroelectric detector was used to measure laser output and harmonic energy. Fundamental transverse mode and a single longitudinal mode laser operation could be attained with proper alignment. The output was linearly polarized, and energy was approximately 30 mJ per pulse.

The observed phase-matching tuning curve shown in Fig. 2 agrees well with that calculated from the dispersion equations. The agreement, particularly in the spacing of the minima and the shape of the secondary maxima, indicates that the interaction length extends over the full crystal length. This in turn is an indication of good crystal optical quality and pump beam parameters within the tolerances of angular acceptance and beam walkoff.

Transverse distribution and total pulse energy of the CO_2 mini-TEA laser were sensitive to alignment. Laser alignment drifted from day to day and was readjusted each time the laser was run. Sometimes the distribution was nearly Gaussian and at other times the distribution, particularly near the focus, showed some ringlike structure. This structure and some accompanying instability were the likely cause of error in these measurements.

The harmonic conversion efficiency and the damage threshold were measured by moving the crystal toward the focus of the pump beam. The energy conversion efficiency versus distance from the beam waist is shown in Fig. 3. The maximum internal energy conversion efficiency was 14%. An analysis of second harmonic generation with modeling of

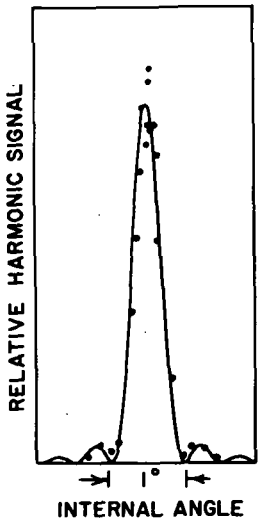

FIG. 2. Phase-matching tuning curve for second harmonic generation of the 10.25-μm R (20) CO_2 laser output in $AgGaSe_2$. The solid curve is calculated from the dispersion equations given in Ref. 2 and the dots are experimental data.

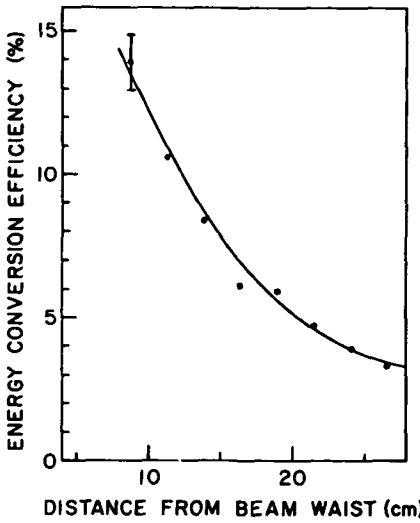

FIG. 3. Internal harmonic energy conversion efficiency as a function of crystal location. The solid curve was calculated assuming Gaussian beam propagation and the dots represent averages of experimental measurements. An error bar is shown for one point.

the pulse profile in time and space shows that energy conversion of the spike was 26% with 35% peak power conversion and 60% peak intensity conversion. The nonlinear optical coefficient derived from this analysis was $d_{36} = 43 \times 10^{-12}$ m/V. This result was within the range of $32.4–57.7 \times 10^{-12}$ m/V of previously reported values.[1-3,13] Energy losses due to Fresnel reflections were not included in internal conversion efficiencies because such reflections can be greatly reduced by antireflection coatings.

Conversion efficiency in this crystal was limited by surface damage which occurred at 12-MW/cm^2 peak intensity or energy fluence of 3 J/cm^2 for the full TEA laser pulse. Damage occurred after about ten shots at these power levels, and it occurred first at the back surface where an antireflection coating would reduce the amplitude of the standing wave.

The growth of $AgGaS_2$ and $AgGaSe_2$ in high-quality, large single crystals, and the demonstration of optical parametric oscillation[9] and efficient second harmonic conversion of the carbon dioxide laser are significant advances in nonlinear infrared frequency conversion. This research is continuing with the planned construction of a $AgGaSe_2$ infrared parametic oscillator and the growth of these materials in larger sizes. Methods of increasing surface damage threshold are also being investigated.

It is likely that these materials will allow the practical use of nonlinear frequency conversion from the visible to wavelengths longer than 10 μm in the near future.

This work was supported in part by the Army Research Office, National Aeronautics and Space Administration, and the Office of Naval Research.

[1]G. D. Boyd, H. M. Kasper, J. H. McFee, and F. G. Storz, IEEE J. Quantum Electron. **QE-8**, 900 (1972).
[2]H. Kildal and J. C. Mikkelsen, Opt. Commun. **9**, 315 (1973).
[3]R. L. Byer, M. M. Choy, R. L. Herbst, D. S. Chemla, and R. S. Feigelson, Appl. Phys. Lett. **24**, 65 (1974).
[4]H. Kildal and T. F. Deutsch, in *Tunable Lasers and Applications*, edited by A. Mooradian, T. Jaeger, and P. Stokseth (Springer, New York, 1976), p. 367.
[5]R. L. Byer, in *Nonlinear Optics*, edited by P. G. Harper and B. S. Wherrett (Academic, San Francisco, 1977), chap. 9.
[6]W. B. Gandrud and R. L. Abrams, Appl. Phys. Lett. **17**, 302 (1970).
[7]D. E. Thompson, J. D. McMullen, and D. B. Anderson, Appl. Phys. Lett. **29**, 113 (1976).
[8]Y. X. Fan, R. C. Eckardt, R. L. Byer, R. K. Route, and R. S. Feigelson, Appl. Phys. Lett. **45**, 313 (1984).
[9]John Feichtner, Westinghouse Research Laboratories, Pittsburgh (private communication).
[10]G. C. Bhar and R. C. Smith, IEEE J. Quantum Electron. **QE-10**, 546 (1974).
[11]G. W. Iseler, J. Cryst. Growth **41**, 146 (1977).
[12]R. K. Route, R. S. Feigelson, R. J. Raymakers, and M. M. Choy, J. Cryst. Growth **33**, 239 (1976).
[13]M. M. Choy and R. L. Byer, Phys. Rev. B **14**, 1693 (1976).

$AgGaS_2$ infrared parametric oscillator

Yuan Xuan Fan,[a] R. C. Eckardt, and R. L. Byer
Applied Physics Department, Stanford University, Stanford, California 94305

R. K. Route and R. S. Feigelson
Center for Materials Research, Stanford University, Stanford, California 94305

(Received 16 March 1984; accepted for publication 21 May 1984)

We report the first operation of an optical parametric oscillator in a chalcopyrite crystal, $AgGaS_2$. Tuning from 1.4 to 4.0 μm is demonstrated for 1.06-μm Nd:yttrium aluminum garnet pumping. The potential tuning range extends to the 12-μm transparency limit of the crystal.

We report on the successful operation of an optical parametric oscillator in $AgGaS_2$. This is the first report of a parametric oscillator in this class of semiconductor chalcopyrite crystals. The potential tuning range of the $AgGaS_2$ parametric oscillator extends to the 12-μm crystal transparency limit.

Crystals belonging to the chalcopyrite symmetry class, $\bar{4}2m$, were proposed as possible infrared tunable parametric oscillator sources as early as 1971.[1,2] The semiconductor chalcopyrite materials are ternary compounds of the form I-III-VI_2 and II-IV-V_2,[3] are birefringent, transparent in the infrared, and have high nonlinear coefficients. Early investigations showed that four chalcopyrite crystals: $AgGaS_2$,[1,2,4] $AgGaSe_2$,[5,6] $ZnGeP_2$,[5,7] and $CdGeAs_2$,[8,9] are phase matchable for nonlinear processes across the infrared. More general information on nonlinear materials and optical parametric oscillation can be found in reviews.[10]

$AgGaS_2$, which is transparent from 0.53 to 12 μm, has been used for infrared generation by mixing,[4,11-13] for infrared up-conversion into the visible,[14,15] and for second harmonic generation of a CO_2 laser.[16] Although the nonlinear coefficient of $AgGaS_2$[2,17] is the smallest of the chalcopyrite crystals,[17] we chose to initiate investigations of $AgGaS_2$ because its visible transparency proved advantageous in crystal growth studies.

The application of chalcopyrite crystals to infrared nonlinear devices and to parametric oscillators has been constrained by crystal growth difficulties.[16] Early crystal

[a] Shangai Institute of Laser Technology, Shanghai, China.

 0003-6951/84/160313-03$01.00

growth work[18–20] showed that problems of cracking, twinning, and nonstoichiometry had to be resolved before useful optical quality crystals could be obtained.[21–24]

Recent growth studies at the Stanford Center for Materials Research have led to significant improvements in crystal quality and size. Currently $AgGaS_2$ crystals are grown by seeded vertical Bridgman method in a sealed fused silica crucible. Seeding to initiate growth along the c axis eliminates cracking and twinning; boules of 2.8 cm diameter by 10 cm in length have been grown with good yield. Following growth the crystals are heat treated in the presence of excess Ag_2S to eliminate absorption and scattering centers.[21]

The growth technique recently has been extended to $AgGaSe_2$ which is a potential candidate crystal for parametric oscillator operation and for second harmonic generation of a CO_2 laser.[6]

We fabricated $AgGaS_2$ crystals 2 cm in length by 1.0×0.5 cm cross section cut at 50.5° to the optical axis in the [110] direction for use in an optical parametric oscillator. $AgGaS_2$ has adequate birefringence to phase match for both type I and type II interactions. We chose to fabricate OPO crystals for type I phase matching for Nd:yttrium aluminum garnet (YAG) pumping at 1.06 μm.

The small birefringence and dispersion of $AgGaS_2$ reduce problems of birefringent walk-off when pumped with a TEM_{00} mode laser source. We used an electro-optic Q-switched Nd:YAG oscillator operating at 10-Hz repetition rate with an 0.69-mm spot size and 20-ns pulse width as a pump source. The pump power was controlled by an attenuator between the pump laser and the OPO.

The $AgGaS_2$ singly resonant oscillator (SRO) used two flat mirrors spaced 3–5 cm apart. The input mirror reflectance was 85%–99% over the 1.4–2.1-μm signal tuning range. The output mirror reflectance varied between 75%–90% over the same spectral range. The $AgGaS_2$ crystal was angle tuned through a 45°–55° range. The crystal surfaces were antireflection coated at 1.6 μm with a single layer of ThF_4.

Figure 1 shows the calculated (line) and measured (dots) tuning curve for $AgGaS_2$ pumped at 1.06 μm. The tuning curve was calculated using Sellmeier equations for the ordinary and extraordinary indices of refraction that were derived by adjusting both ultraviolet and infrared poles independently for the two indices to obtain a least squares fit to the dispersion data of Boyd *et al.*[2] These Sellmeier equations are

$$n_0^2 = 3.3970 + \frac{2.3982}{1-0.09311/\lambda^2} + \frac{2.1640}{1-950.0/\lambda^2}$$

and

$$n_e^2 = 3.5873 + \frac{1.9533}{1-0.11066/\lambda^2} + \frac{2.3391}{1-1030.7/\lambda^2}, \quad (1)$$

where λ is the wavelength in μm.

Predicted phase matching angles approximately one degree larger than the experimental values are obtained with previously published dispersion equations.[25,26] Equation (1) gives better agreement with the measured angles. The differences in these equations are probably caused by fitting to different portions of the dispersion data. Index of refraction measurements need to be made on currently available high optical quality crystals to improve the dispersion equations.

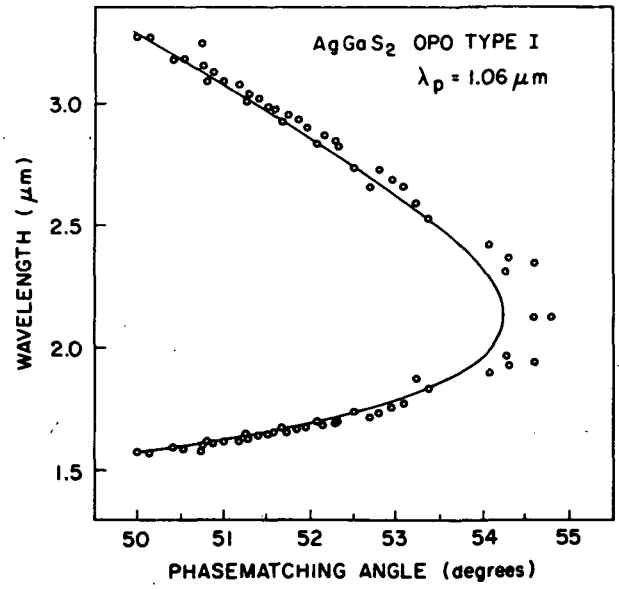

FIG. 1. Calculated (line) and measured tuning range (dots) for a 1.06-μm pumped type I angle phase matched $AgGaS_2$ parametric oscillator.

The $AgGaS_2$ OPO threshold is measured to be 1.5 mJ of incident 1.06-μm energy. This corresponds to 1.15-mJ incident pump energy just inside the crystal surface. The threshold of a pulsed SRO can be calculated using the results of Brosnan and Byer.[27] The threshold energy density is given by

$$J_0 = \frac{2.25\tau}{\kappa g_s \mathscr{L}^2}\left(\frac{L}{2\tau c}\ln\frac{P_n}{P_0} + 2\alpha l + \ln\frac{1}{\sqrt{R}} + \ln 2\right)^2,$$

where

$$\kappa = 2\omega_s\omega_i d_{\text{eff}}^2/n_s n_i n_p \epsilon_0 c^3. \quad (2)$$

The definitions of the parameters are the same as given in Ref. 27. The mode coupling coefficient is $g_s = w_p^2/(w_p^2 + w_s^2)$ and the effective parametric gain length is $\mathscr{L} = l_w \operatorname{erf}(\sqrt{\pi} l/2l_w)$, where l_w is the walk-off length and l the crystal length. Here L is the optical length of the cavity, τ the pump pulse width, P_n/P_0 the ratio of signal power to noise power at threshold, and R the product of mirror reflectivities.

Threshold energy was calculated using Eq. (2) with parameters representative of our experimental conditions. The $AgGaS_2$ nonlinear coefficient for 10.6 μm: $d_{36} = 18\times10^{-12}$ m/V given by Kurtz *et al.*,[16] was used. For $\lambda_p = 1.064$ μm and $\lambda_s = 2.128$ μm, the value of $d_{36} = 22\times10^{-12}$ m/V was obtained using the constant Miller's delta condition. For type I phase matching $d_{\text{eff}} = d_{36}\sin\theta = 18\times10^{-12}$ m/V. Using $L = 5.8$ cm, $l = 2.0$ cm, $\alpha = 0.01$ cm^{-1}, $R = 0.80$, and $\tau = 20$ ns, we calculate a threshold energy of 0.94 mJ for a spot size of $w_p = 0.69$ mm. The calculated and measured thresholds are in good agreement, giving further indication of the excellent optical quality of the $AgGaS_2$ crystals.

The $AgGaS_2$ parametric oscillator generated 0.5 mJ output energy when pumped at 1.2 times above threshold with the pump spot size increased to $w_p = 1.7$ mm. The corresponding energy conversion efficiency was 16%. The OPO output pulse width was 18 ns and followed the pump pulse

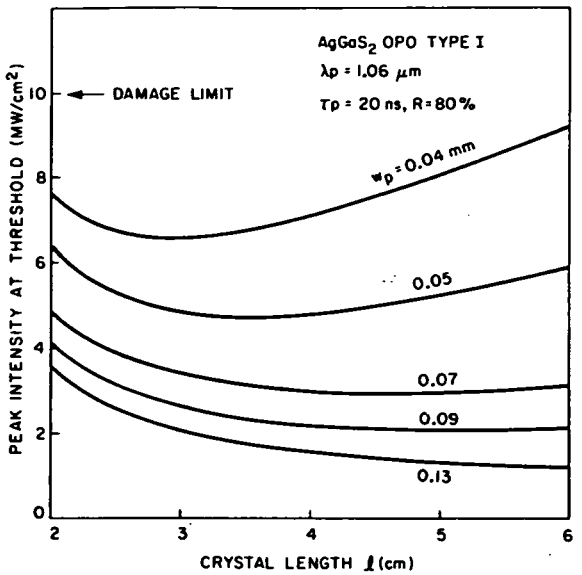

FIG. 2. Calculated threshold intensity vs crystal length with pump spot size as the parameter. The measured damage intensity is 10 MW/cm^2 for a 20-ns, 1.06-μm source.

width as expected. Operation further above threshold was not possible due to crystal surface damage caused by the resonated signal wave intensity within the SRO cavity. Oscillation was observed at wavelengths as long as 4.0 μm. These data are not shown in Fig. 1 because crystal orientation was not recorded. At wavelengths longer than 4.0 μm, parametric oscillator threshold could not be reached because of surface damage.

We carefully measured the $AgGaS_2$ surface damage intensity for 20-ns pulses at 1.06 μm. The damage intensity was 13 MW/cm^2 for 100 pulses and 10 MW/cm^2 for 1000 pulses at 10-Hz repetition rate. Attempts to increase the damage threshold by applying antireflection coatings to the crystal surface were not successful. Improvement of the surface damage intensity is important for future nonlinear devices that utilize $AgGaS_2$ or related crystals. Considerable work needs to be done to understand the reasons for the low damage threshold intensity of $AgGaS_2$.

For stable long term operation the $AgGaS_2$ SRO threshold must be reduced. A step in this direction is to increase the crystal length from 2 to 4 cm by the growth of larger diameter boules. Other factors can also be adjusted to decrease the OPO threshold intensity.[28] These factors include increasing the pump spot size, reducing the pump pulse width, and reducing the OPO cavity length.

Figure 2 shows the calculated OPO threshold intensity versus crystal length with the pump spot size as the parameter. The combination of longer crystals and larger pump spot sizes leads to a threshold reduction from the current value of 5 to less than 1.5 MW/cm^2.

In conclusion, we have demonstrated the first optical parametric oscillator in a chalcopyrite crystal $AgGaS_2$. Improvements in the growth of $AgGaS_2$ and the closely related crystal $AgGaSe_2$ should allow parametric oscillator operation across the infrared wavelength range to 18 μm. These crystals will also have applications in second harmonic generation of CO_2, up-conversion, and infrared generation by mixing.

This work was supported by the Army Research Office, National Aeronautics and Space Administration, the Stanford University Center for Materials Research, S.R.I. International and Spectra Physics.

[1]D. S. Chemla, P. J. Kupecek, D. S. Robertson, and R. C. Smith, Opt. Commun. **3**, 39 (1971).
[2]G. D. Boyd, H. Kasper, and J. H. McFee, IEEE J. Quantum Electron. **QE-7**, 563 (1971).
[3]N. A. Goryunova, S. M. Ryvkin, I. M. Fishman, G. P. Shpen'kov, and I. D. Yaroshetskii, Sov. Phys. Semicond. **2**, 1272 (1965); N. A. Goryunova, *The Chemistry of Diamond-Like Semiconductors* (MIT, Cambridge, MA, 1965).
[4]D.C. Hanna, V. V. Rampal, and R. C. Smith, Opt. Commun. **8**, 151 (1973).
[5]G. D. Boyd, H. M. Kasper, J. H. McFee, and F. G. Storz, IEEE J. Quantum Electron. **QE-8**, 900 (1972).
[6]R. L. Byer, M. M. Choy, R. L. Herbst, D. S. Chemla, and R. S. Feigelson, Appl. Phys. Lett. **24**, 65 (1974).
[7]G. D. Boyd, E. Buehler, and F. G. Storz, Appl. Phys. Lett. **18**, 30 (1971).
[8]R. L. Byer, H. Kildal, and R. S. Feigelson, Appl. Phys. Lett. **19**, 237 (1971).
[9]G. D. Boyd, E. Buehler, F. G. Storz, and J. H. Wernick, IEEE J. Quantum Electron. **QE-8**, 419 (1972).
[10]R. L. Byer, "Optical Parametric Oscillators," in *Quantum Electronics: A Treatise, Vol. I: Nonlinear Optics, Part B*, edited by H. Rabin and C. L. Tang (Academic, New York, 1975), p. 588.
[11]D. C. Hanna, V. V. Rampal, and R. C. Smith, IEEE J. Quantum Electron. **QE-10**, 461 (1974).
[12]R. J. Seymour and F. Zernike, Appl. Phys. Lett. **29**, 705 (1976).
[13]J. J. Jacob, SPIE Proc. **461**, 11 (1984).
[14]E. S. Voronin, V.S. Solomartin, N. I. Cherepov, V.V. Shuvalov, V. V. Badikov, and O. N. Pivovazov, Sov. J. Quantum Electron. **5**, 597 (1975).
[15]W. Jantz and P. Koidl, Appl. Phys. Lett. **31**, 99 (1977).
[16]P. J. Kupecek, C. A. Schwartz, and D. S. Chemla, IEEE J. Quantum Electron. **QE-10**, 546 (1974).
[17]S. K. Kurtz, J. Jerphagnon, and M. M. Choy, in Landolt–Bornstein, New Series, Group III, Vol. 11, *Elastic Piezo-electric, Pyro-electrick, Piezo-optic, Electro-optic Constants and Nonlinear Dielectric Susceptibilities of Crystals*, edited by K. H. Hellwege and A. M. Hellwege (Springer, New York, 1979), Chap. 6, p. 671.
[18]S. C. Abrahams and J. L. Bernstein, J. Chem. Phys. **59**, 1625 (1973).
[19]P. Korczak and C. B. Staff, J. Cryst. Growth **24/25**, 386 (1974).
[20]R. K. Route, R. S. Feigelson, and R. J. Raymakers, J. Cryst. Growth **24/15**, 390 (1974); **33**, 239 (1976).
[21]R. K. Route, R. S. Feigelson, R. J. Raymakers, and M. M. Choy, J. Cryst. Growth **33**, 239 (1976).
[22]H. Matthes, R. Viehmann, and N. Marschall, Appl. Phys. Lett. **26**, 237 (1975).
[23]J. C. Mikkelsen, Jr. and H. Kildal, J. Appl. Phys. **49**, 426 (1978).
[24]H. J. Bordeleben, A. Goltzenc, C. Schwab, and R. S. Feigelson, Appl. Phys. Lett. **32**, 741 (1978).
[25]G. C. Bhar and R. C. Smith, IEEE J. Quantum Electron. **QE-10**, 546 (1974).
[26]S. H. Wemple, J. D. Gabbe, and G. D. Boyd, J. Appl. Phys. **46**, 3597 (1975).
[27]S. J. Brosnan and R. L. Byer, IEEE J. Quantum Electron. **QE-15**, 415 (1979).
[28]Y. X. Fan and R. L. Byer, SPIE Proc. **461**, 27 (1984).

Reprinted from SPIE Vol. 461—New Lasers for Analytical and Industrial Chemistry

Progress in optical parametric oscillators

Fan, Yuan Xuan* and R.L. Byer

Applied Physics Department, Stanford University,
Stanford, California 94305

Abstract

We review the current status of parametric oscillator tunable sources with an emphasis on progress in the past decade. Recent results are reported for the first OPO operated in a chalcopyrite crystal, $AgGaS_2$.

Tunable coherent sources are very useful for many applications including spectroscopy, chemistry, combustion diagnostics and remote sensing. The ideal tunable laser should offer a wide tuning range, high output power, high conversion efficiency, narrow bandwidth and good amplitude and frequency stability. Compared with other tunable sources, optical parametric oscillators (OPO) offer the potential advantage of a wide wavelength operating range that extends from 0.2 μm to 25 μm limited only by the transparency range of the nonlinear crystals. Furthermore, the OPO tuning range is not limited by a gain-bandwidth product so that a single device can tune from 1.4 - 10 μm for example.

Figure 1 shows the tuning range of parametric oscillators and tunable optical sources. Only diode lasers offer the potential for extended tunability in a single device. Dye lasers, while widely used, suffer from limited tuning for each dye and from operation wavelengths in the 3 - 1.3 μm region. Fortunately, dye laser tuning can be extended by nonlinear processes into the ultraviolet and near infrared region.

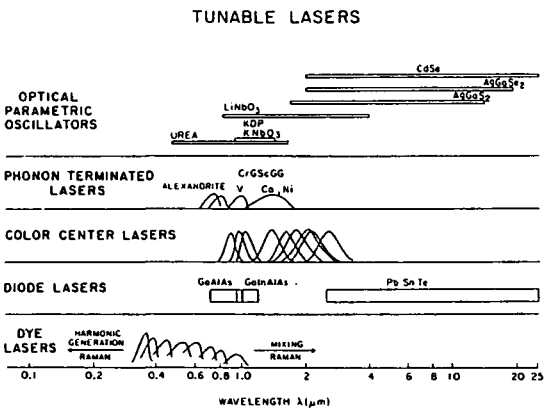

Fig.1--Overview of tunable laser sources Parametric oscillators offer wide tuning ranges from 0.4 to beyond 25 μm.

Parametric oscillators also offer the potential reliability of an all solid state source. For example, early $LiNbO_3$ parametric oscillators sold commercially by Chromatix in 1970 are still operating today with the same crystal. Parametric oscillators also offer high peak power and high conversion efficiency. Bandwidth control of parametric oscillators is similar to that required for dye lasers. Finally, the parametric process is ideal for amplification since the parametric gain is polarized, forward directed and bandwidth limited, thus avoiding superfluorescence problems associated with dye laser amplifiers.

The problems that have prevented wide use of parametric oscillators are crystal surface damage, crystal photorefractive response, crystal size and optical quality. In addition, parametric oscillators, unlike dye lasers, require diffraction limited pump radiation. The development of suitable laser pump sources has held back OPO use.

Since the first optical parametric oscillator demonstration in 1965 by Giordmaine and Miller[1] in $LiNbO_3$, many devices have been demonstrated in a variety of nonlinear materials. Table I presents a brief summary of parametric oscillator progress from 1965 to 1980. In 1966 Akhmanov et.al.,[2] first used KDP as an OPO crystal . Bjorkholm[3] demonstrated the first singly resonated OPO with a $LiNbO_3$ crystal pumped by a ruby laser in 1968. In the same year a cw OPO (DRO) was operated in infrared using $BaNaNb_5O_{15}$ crystal by Smith et.al.,[4] and in visible using a $LiNbO_3$ crystal by Byer et.al.[5] In 1972 Herbst and Byer[6] operated the first infrared OPO using CdSe as the nonlinear crystal. $LiIO_3$ and Ag_3AsS_3 OPO's were demonstrated in 1973 by Nath and Pauli[7] and Hanna et.al.[8] The first picosecond OPO using $LiNbO_3$ appeared in 1974 by Laubereau et.al.,[9] In the same year Massey and Elliott[10] demonstrated a CDA OPO. Dikchyus et.al.,[11] demonstrated an OPO using α-HIO_3 in 1975. Kato[12] used $KNbO_3$ as an OPO crystal in 1981. 1983 saw the demonstration of OPO's using Urea and $AgGaS_2$ by Donaldson and Tang[13] and by Fan and Byer.[14]

*Current address: Shanghai Institute for Laser Technology, Shanghai, China.

TABLE I

History of OPO Devices

1965	First OPO demonstration ($LiNbO_3$)	Giordmaine/Miller
1966	KDP OPO	Akhmanov et.al.
1968	First SRO OPO ($LiNbO_3$)	Bjorkholm
1968	First cw OPO (BSN)	Smith et.al.
1968	cw OPO in visible ($LiNbO_3$)	Byer et.al.
1972	CdSe OPO	Herbst/Byer
1973	$LiIO_3$ OPO	Nath/Pauli
1973	Ag_3AsS_3 OPO	Hanna/Smith
1974	First PS OPO ($LiNbO_3$)	Laubereau et.al.
1974	CDA OPO	Massey/Elliott
1975	α-HIO_3 OPO	Dikchyus
1981	$KNbO_3$ OPO	Kato D'yakov et.al.
1983	Urea OPO	Donaldson/Tang
1983	$AgGaS_2$ OPO	Fan/Byer

TABLE II
RECENT SELECTED OPO EXPERIMENTS

Crystal	Pump laser	Pump pulsewidth	Tuning range	Conversion efficiency	Authors
KDP	Nd:YAG 0.53 µm	30 ps	0.9 - 1.3 µm	50%	Kabelka et.al./Piskarskas (1979)
$LiNbO_3$	Nd:YAG unstable resonator 1.06 µm	10 ns	1.4 - 4.0 µm	10%	Baumgartner/Byer (1979)
$KNbO_3$	Nd:YAG 0.532 µm	10 ns	0.88 - 1.35 µm	75%	Kato (1982)
UREA	Nd:YAG 0.3547 µm	10 ns	0.49 - 128 µm	25%	Donaldson/Tang (1983)
$AgGaS_2$	Nd:YAG	20 ns	1.4 - 4.0 - 10 µm	16%	Fan/Byer (1983)
Ti:$LiNbO_3$ Waveguide	Dye	60 ns	Amplifier		Sohler/Suche (1980)
Vitreous Si Fiber	Nd:YAG	Mode locked Q-switched	0.52 - 1.63 µm	25%	Hill et.al. (1980)

Review papers summarizing progress in parametric oscillators have been written by Harris[15] in 1969, by Byer[16] in 1973 and by Smith[17] in 1974.

In this paper we concentrate on optical parametric oscillator progress that has taken place since 1973.

During the past decade experiments have been carried out to improve parametric oscillator performance and to solve the crystal growth and damage problems. Table II lists the significant experiments since 1973.

We first note the progress in picosecond OPO's. Work by the Piskarskas group has been done on picosecond parametric oscillators in the Soviet Union and by Kaiser in Germany which has led to significant advances in picosecond OPO performance. The picosecond OPO is a useful source for the investigation of fast processes in the areas of physics, chemistry, electronics and biology. Using a KDP crystal pumped by the second harmonic of a 30 psec Nd:YAG laser, OPO conversion efficiencies as high as 50% have been reached.[18] Pulsewidths as short as 0.5 ps have been demonstrated using a $LiNbO_3$ OPO pumped by 1.06 µm.[19] The frequency linewidth has been narrowed to the Fourier transform limit for a $LiIO_3$ parametric oscillator pumped at 0.532 µm.[20]

A breakthrough in nanosecond parametric oscillators made use of an unstable resonator Nd:YAG laser to pump an angle tuned $LiNbO_3$ parametric oscillator by Baumgartner and Byer.[21] The $LiNbO_3$ crystal was grown in the 01.4 direction[22] which is close to the optimum direction for Type I phasematching when pumped at 1.06 µm. From this parametric oscillator 6 mJ per pulse at 10 Hz with a linewidth of 3 cm^{-1} or 4 mJ per pulse with a linewidth of 0.2 cm^{-1} in the tuning range of 1.4 - 4 µm was obtained.

The first demonstration of a waveguide[23] and fiber[24] parametric amplification and generation have recently been obtained. These approaches represent new directions in parametric oscillation studies.

Along with crystal growth progress of known materials, new crystals such as $KNbO_3$[12], Urea[13] and $AgGaS_2$[14] have been demonstrated as optical parametric oscillators.

Materials are critical to optical parametric oscillator performance. A review paper by Nikogosayan[25] summarizes the properties of 20 nonlinear crystals. Table III is a list of important parametric oscillator crystals. However, in addition to the crystals listed, other crystals have been used for parametric generation including $LiIO_3$[7,20,26,27,29] $KNbO_3$[12,30], $BaNaNb_5O_{15}$[31,32], Ag_3AsS_3[8,33], CdSe[6,34-37], CDA[5] and α-HIO_3.[11,28,38] KDP is a well known nonlinear crystal and has been often used for parametric oscillator studies.[18,20,39,41] The nonlinear coefficient parametric gains listed in Table III are relatively to KDP. $LiNbO_3$ is the most widely used crystal for both nanosecond[21,29,42-46] and picosecond[9,19,47-53] parametric oscillators. The $LiNbO_3$ parametric oscillator followed by a parametric amplifier has provided 85 mJ per pulse output at 10 Hz. The output power limitation was set by the 20 mm x 60 mm crystal size and surface damage. For visible pumping of $LiNbO_3$, the induced photorefractive phenomenon has led to high optical loss and to poor nonlinear conversion efficiency. Efforts are continuing toward understanding the cause of the damage and to eliminate it.[54]

Urea has received attention because its UV transparency range and nonlinear coefficient that is a factor of 2 larger than KDP. As an example, Fig. 2 shows the calculated Type I phasematching tuning curve of a Urea OPO pumped by the third and fourth harmonic of a Nd:YAG laser. Recently Urea pumped by the third harmonic of Nd:YAG has operated as a

TABLE III

Representative Parametric Oscillator Crystals

Crystal	Relative nonlinear coefficient	Transparency range	Normalized parametric gain at 1 MW/cm²	Damage threshold
KDP	1	0.2 - 1.3 μm	1(0.26 μm)	1 GW/cm²
Urea	2	0.21 - 1.8 μm	2(0.35 μm)	1 GW/cm²
$LiNbO_3$	10	0.35 - 4.5 μm	50(0.53 μm)	80 MW/cm²
$AgGaS_2$	40	0.54 - 12 μm	400(1.06 μm)	10 - 20 MW/cm²
$AgGaSe_2$	80	0.8 - 18 μm	800(2 μm)	10 - 20 MW/cm²

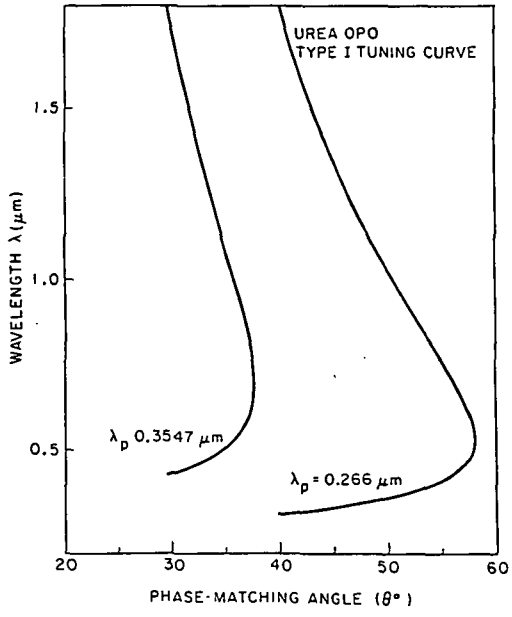

Fig. 2--Calculated Type I Urea OPO tuning curves for 0.3547 and 0.266 μm pump wavelengths.

visible OPO.[13]

The large nonlinear coefficients and extended infrared transparency ranges make chalcopyrite crystals an important class. There are four useful crystals in this family: $CdGeAs_2$, $ZnGeP_2$, $AgGaSe_2$ and $AgGaS_2$. $CdGeAs_2$ and $ZnGeP_2$ have nonlinear coefficients 50 to 20 times higher than $LiNbO_3$, but are very difficult to grow. We have iniated growth studies of $AgGaS_2$ and $AgGaSe_2$. Recently we have grown high optical quality $AgGaS_2$ boules and have fabricated 2 cm long OPO crystals for use in a near infrared parametric oscillator.[15] The $AgGaS_2$ OPO has 0.5 mJ output for a conversion efficiency of 16% when pumped 1.2 times above threshold by 1.06 μm from a Q-switched Nd:YAG source. Figure 3 shows the calculated tuning curve along with experimental data for this $AgGaS_2$ OPO.

$AgGaS_2$ and $AgGaSe_2$ are phasematchable for both Type I and Type II interactions. As an example of the potential infrared tuning range, Fig. 4 shows the calculated Type I tuning curve for an $AgGaSe_2$ OPO pumped at 2 μm. An appropriate pump source may be the $Co^{++}:MgF_2$ laser operated by Moulton. A very impressive feature of this tuning curve is the possibility of tuning the entire range from 2.3 μm to 18 μm using only a single crystal.

Table IV shows the calculated energy and intensity thresholds for $AgGaS_2$ and $AgGaSe_2$ parametric oscillators relative to $LiNbO_3$. $AgGaS_2$ and $AgGaSe_2$ have much lower OPO thresholds and offer a wider tuning range than $LiNnO_3$. However, their low damage intensity, shown in Table III, requires the use of 4 cm long crystals for reliable parametric oscillator operation.

In the past, theoretical work has been done to understand the factors affecting the parametric oscillator performance. The most studied factors are those which could increase conversion efficiency and reduce parametric oscillator threshold. Low threshold is desired especially for crystals having low damage intensity, such as $AgGaS_2$.

Previous studies have considered methods to reduce the energy threshold.[57-60] However, the threshold peak power density may be increased as the energy threshold is reduced.

Methods of reducing OPO threshold such as elliptical focusing[56] have been previously suggested. Factors that affect parametric oscillation threshold include resonator length, the ratio of resonator length and crystal length, mirror reflectance, pump pulse width, pump beam spot size and crystal length. In general, a shorter resonator length produces lower OPO threshold. High reflectance of the OPO output mirror also reduces the threshold peak power density. However, the intercavity signal peak power density increased with increasing reflectance. The intercavity signal peak power density may increase to become many times higher than pump peak power density for low output coupling. Thus an optimum mirror reflectance for the lowest peak power density of the pump and intercavity signal must be found. Increasing pump pulse width also reduces the OPO threshold peak power density. On the other hand, if the crystal surface damage is caused by impurity absorption, then the damage intensity is proportional to the inverse square root of pulse width. Thus pulsewidths as short as possible without the onset of small scale self-focusing or increased threshold intensities due to OPO build-up times are desired.

Figure 5 is an example of a calculated $AgGaS_2$ OPO threshold vs crystal length with pump beam spotsize as the parameter. Longer crystals and large spot sizes decrease the OPO

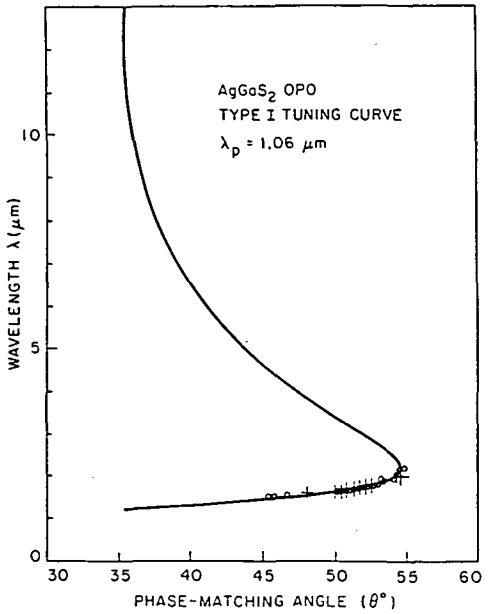

Fig. 3--Calculated and measured $AgGaS_2$ OPO tuning curve for 1.06 μm pumping.

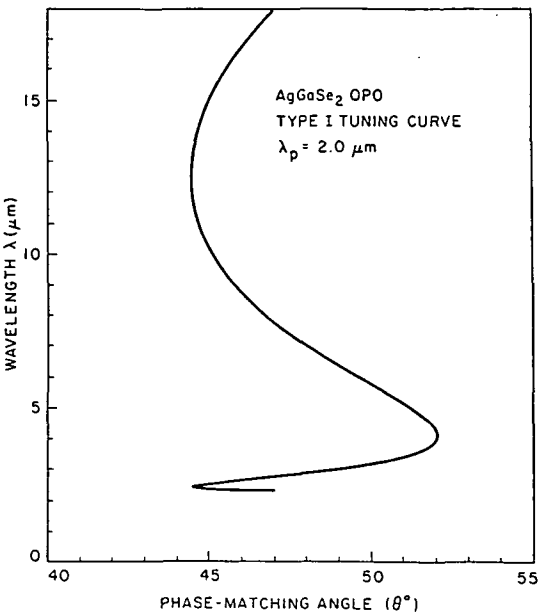

Fig. 4--Calculated $AgGaSe_2$ Type I OPO tuning curve for a 2.0 μm pump wavelength. Operation to 18 μm is projected using a single crystal cut at 48°.

TABLE IV
OPO Threshold

Crystals	Energy threshold	Power density threshold
$AgGaSe_2$ (λ_p = 2 μm)	0.46 mJ	3.0 MW/cm^2
$AgGaS_2$ (λ_p = 1.06 μm)	0.9 mJ	5.7 MW/cm^2
$LiNbO_3$ (λ_p = 0.659 μm)	2.5 mJ	16.5 MW/cm^2

Operating Conditions:

Pump width	τ_p = 20 ns
Pump beam radius	w_p = 0.7 mm
Crystal length	ℓ = 2 cm
Mirror reflectance	R = 80%

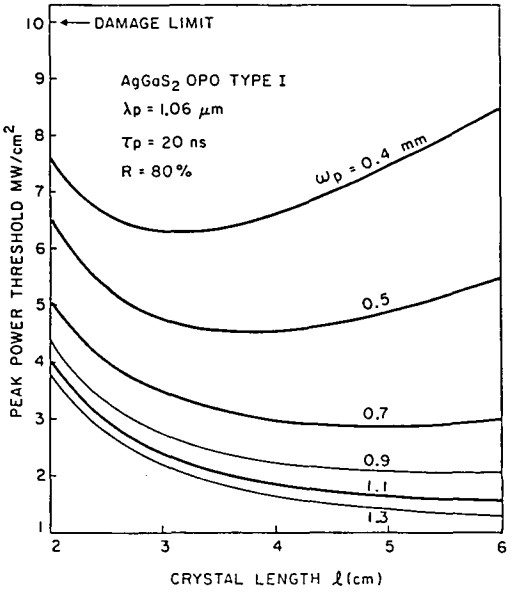

Fig. 5--Calculated $AgGaS_2$ OPO threshold intensity vs crystal length with pump spot size ω_p as a parameter. The OPO has operated for a 2 cm crystal length at ω_p = .69 mm. A threshold intensity reduction of four is projected for 4 cm crystal lengths.

threshold intensity. If the limitation on parametric oscillator operation is the crystal damage power density, then a larger beam spot and more uniform intensity distribution is preferred. For example, a 4 cm long, $AgGaS_2$ crystal with a 1 mm pump beam radius, yields a calculated $AgGaS_2$ OPO threshold of 2 MW/cm^2 which is well below the measured crystal damage threshold of 10 MW/cm^2. We are working toward the growth of longer, high optical quality $AgGaS_2$ and $AgGaSe_2$ crystals.

Optical parametric oscillators have been used for many applications in the past decade. Picosecond parametric oscillators have been used for selective excitation of molecular levels.[61-69] For example, Magnitskii and Tunkin[70] measured dephasing times using $LiNbO_3$

parametric oscillators pumped by Nd:YAG laser pulses with 40 ps pulsewidth. OPO's have also been used for infrared remote sensing of the atmosphere. Byer et.al.,[70-73] measured SO_2, CH_4 and water vapor in the atmosphere. The atmospheric temperature and humidity were also measured using an unstable resonator Nd:YAG pumped computer-controlled angle-tuned $LiNbO_3$ parametric oscillator. Optical parametric oscillators also have been used for absorption spectroscopy,[73-76] dispersion measurements[77-79] and bacterial photosynthesis.[80]

In conclusion, impressive progress in optical parametric oscillators has been made in the past decade. Parametric oscillators are an all-solid state tunable source with a wide tuning range from the uv to far infrared. OPO's offer diffraction limited beam quality, high peak power on the order of tens of MW and average power on the order of watts. Conversion efficiencies of more than 40% have been demonstrated for singly resonated parametric oscillators. Linewidths have been narrowed to 0.001 cm^{-1} with an etalon and computer controlled frequency tuning has been demonstrated over a 1.4 - 4.0 μm range.

With further development of nonlinear crystals and diffraction limited pump laser sources, parametric oscillators should find wide application as sources of tunable coherent radiation.

References

1. Giordmaine, J.A., Miller, R.C., Phys. Rev. Letts. vol. 14, p.973, 1965.
2. Akhmanov, S.A., Kovrigin, A.I., Kolosov, V.A., Piskarskas, A.I., Kolosov, V.A., Piskarskas, A.S., Fadeev, V.V., Khokhlov, R.V., JEPT Letts. vol. 3, p.241, 1966.
3. Bjorkholm, J.E., Appl. Phys. Letts. vol. 13, 53; p.399, 1968.
4. Smith, R.G., Geusic, J.E., Levinstein, H.J., Singh, S., van Uitert, L.G., J. Appl. Phys. vol. 39, p.4030, 1968 ; Appl. Phys. Letts. vol. 12, p.308, 1968.
5. Byer, R.L., Oshman, M.K., Young, J.F., Harris, S.E., Appl. Phys. Letts. vol. 13, p. 109, 1968.
6. Herbst, R.L., Byer, R.L., Appl. Phys. Letts. vol. 21, p.189, 1972.
7. Nath, G., Pauli, G., Appl. Phys. Letts. vol. 22, p.75, 1973.
8. Hanna, D.C., Davies, B.L., Smith, R.C., Appl. Phys. Letts. vol. 22, p.440, 1973.
9. Laubereau, A., Greiter, L., Kaiser, W., Appl. Phys. Letts., vol. 25, p.87, 1974.
10. Massey, G.A., Elliott, R.A., IEEE Journ. Quant. Electr. vol. QE-10, p.899, 1974.
11. Dikchyus, G.A., Kabelka, V.I., Piskarskas, A.S., Stabinis, A. Yu., Sov. Journ. Quant. Electr. vol. 4, p.1402, 1975.
12. Kato, K., IEEE Journ. Quant. Electr. vol. QE-18, p.451, 1982.
13. Donaldson, W., Tang, C.L., CLEO 1983. Conference Paper. Appl.Phys.Letts. vol. 44, p.25, 1984.
14. Fan, Y.X., Byer, R.L., CLEO 1983 Conference Paper.
15. Harris, S.E., Proc. IEEE, vol. 57, p.2096, 1969.
16. Byer, R.L., "Optical Parametric Oscillators" in Quantum Electronics:A Treatise, vol.1 part B, ed. by Rabin, H., Tang, C.L., 1975.
17. Smith, R.G., Chapter 4 in Lasers, vol. 4, Levine & DeMaria, eds. 1976.
18. Kabelka, V., Kutka, A., Piskarskas, A., Smil'gyavichyus, V., Yasevichyute, Ya., Sov. Journ. Quant. Elect. vol. 9, p.1022, 1979.
19. Fendt, A., Kranitsky, W. Laubereua, A., Kaiser, W., Opt. Commun. vol. 28, p.142,1979.
20. Banin, A.A., Belyaev, Yu, N., Verevkin, Yu, K., Freidman, G.I., Sov. Journ. Quant. Electr. vol. 9, p.728 1979.
21. Baumgartner, R., Byer, R.L., Proc. SPIE, vol. 95, p.92 1976.
22. Byer, R.L., Herbst, R.L., Feigelson, R.S., Kway, W.L., Opt. Commun. vol. 12. p.427, 1974.
23. Sohler, W., Suche, H., Appl. Phys. Letts. vol. 37, p.255, 1980.
24. Hill, K.O., Kawasaki, B.S., Fujii, Y., Johnson, D.C., Appl. Phys. Letts. vol. 36, p.888, 1980.
25. Nikogosyan, D.N., Sov. Journ. Quant. Electr. vol. 7, p.1, 1977.
26. Weisman, R.B., Rice, S.A., Opt. Commun. vol. 19. p.28, 1976.
27. Banin, A.A., Belyaev, Yu, N., Petryakov, V.N., Sushchik, M.M., Freidman, G.I., Sov. Jurn. Quant. Electr. vol. 6, p.613, 1976.
28. Danelyus, R., Dikchyus, G., Kabelka, V., Piskarskas, A., Stabinis, A., Yasevichyute, Yu., Sov. Journ. Quant. Electr. vol. 7, p.1360, 1977.
29. Volosov, V.D., Krylov, V.N., Opt. and Spectr. vol. 51, p.519, 1981.
30. D'yakov, V.A., Pryalkin, V.I. Kholodnykh, A.I., Sov. Journ. Quant. Electr. vol. 11, p.433, 1981.
31. Baryshev, S.A., Pryakin, V.I., Kholodnykh, A.I., Sov. Techn. Phys. Letts. vol. 6, p. 415, 1980.
32. Soldatov, A.N., Sukhanov, V.B., Polunin, Yu, P., Kholodnykh, A.I., Sov. Phys. Techn. vol. 26, p.517, 1981.
33. Elsaesser, T., Seilmeier, A., Kaiser, W., Opt. Commun. vol. 44, p.293, 1983.
34. Davydov, A.A., Kulevskii, L.A., Prokhorov, A.M., Savel'ev, A/D., Smirnov, V.V., Opt. Commun. vol. 9, p.234, 1973.
35. Weiss, J.A., Goldberg, L.S., Appl. Phys. Letts. vol. 24, p.389, 1974.
36. Wenzel, R.G. Arnold, G.P., Appl. Optics, vol. 15, p.1322, 1976.

37. Levinos, N.J., Arnold, G.P., IEEE Journ. Quant. Electr. vol. QE-13, #8, 58D, 1977.
38. Dikchyus, G., Andelyus, R., Kabelka, V., Piskarskas, A., Tomkyavichyus, T., Stabinis, A., Sov. Journ. Quant. Electr. vol. 6, #4, p.525, 1976.
39. Bareika, B., Dikchyus, G., Isyanova, E.D., Piskarskas, A., Sirutkaitis, V., Sov. Techn. Phys. Letts. vol. 6, p.301, 1980.
40. Gadonas, R., Danelyus, R., Piskarskas, A., Sov. Journ. Quant. Electr. vol. 11, p.407, 1981.
41. Bergner, H., Bruckner, V., Schroder, B., Sov. Journ. Quant. Electr. vol. 11, p.952, 1981 ; Opt. Acta, (G.B.), vol. 29, p. 1491, 1982.
42. Pearson, J.E., Yariv, A., Ganiel, V., Appl. Opt. vol. 12, p.1165, 1973.
43. Herbst, R.L., Fleming, R.N., Byer, R.L., Appl. Phys. Letts., vol. 25, p.520, 1974.
44. Mishchenko, V.A., Myl'nikov, G.D., Soholenko, D.N., Sov. Journ. Quant. Electr. vol. 9, p.80, 1979.
45. Marunkov, A.G., Pryalkin, V.I., Kholodnykh, A.I., Sov. Journ. Quant. Electr. vol. 11, p.869, 1981.
46. Tanako, Y., Kushida, T., Shionoya, S., Opt. Commun. vol. 25, p.273, 1978.
47. Kushida, T., Tanada, Y., Ujima,M., Jap. J. Appl. Phys. vol. 16, p.2227, 1977.
48. Ivanova, Z.I., Kabelka, V., Magnitskii, S.A., Piskarskas, A., Smil'gyavichyus,V., Rubinina, N.M., Tunkin, V.G. Sov. Journ. Quant. Electr. vol. 7, p.1414, 1977.
49. Seilmeier, A., Spanner, K., Laubereau, A., Kaiser, W., Opt. Commun. vol. 24, p.237, 1978.
50. Liu, P.L. Appl. Opt. vol. 18, p.3543 & 3545, 1979.
51. Campillo, A.J., Hyer, R.C., Shapiro, S.L. Opt. Letts. vol. 4, p.325, 1979.
52. Kranitsky, W., Ding, K., Seilmeier, A., Kaiser, W., Opt. Commun. vol. 34, p.483,1980 .
53. Tanaka, Y., Kuroda, H., Shionoya, S., Opt. Commun. vol. 41, p.434, 1982.
54. Byer, R.L., Park, Y.K., Appl. Phys. Letts. vol. 39, p.17, 1981.
55. Fan, Y.X., Byer, R.L., "$AgGaS_2$ Infrared Parametric Oscillator", to be published.
56. Kuizenga, D.J. Appl. Phys. Letts. vol. 21, p.570, 1972.
57. Fisher, R., Nickles, P.V., Chu, T.B., Wieczorek, L.W., Ann. Phys. y, Folge, Band. 39, Heft. 4, p.287, 1982.
58. Dzhotyan, G.P., D'yakov, Yu, E., Sov. Journ. Quant. Electr. vol. 7, p.1337, 1977.
59. Guha, S., Wu, F.J., Falk, J., IEEE Journ. Quant. Electr. vol. QE-18, 907, 1982.
60. Leone, S.R., Moore, C.B., Chem. Phys. Letts. (Netherlands), vol. 19, p.340, 1973.
61. Barnes, R.H., Moeller, C.E., Kircher, J.F., Verber, C.M., Appl. Phys. Letts. vol. 24, p.610, 1974.
62. Herdvik, A., Sackett, P.B., Appl. Opt., vol. 13, p.1060, 1974.
63. Akhmanov, S.A., J. Raman Spectr. (Netherlands), vol. 2, p.239, 1974.
64. Kryukov, P.G., Matveets, Yu, A., Nikogosyan, D.N., Sharkov, A.V., Sov. Journ. Quant. Electr. vol. 8, p.1319, 1978.
65. Hager, J., Journ. Chem. Phys. vol. 70, p.2859, 1978 ; Journ. Chem. Phys. vol. 72, p.4286, 1980.
66. Dash, C.J. Moore, C.B., Journ. Chem. Phys. vol. 72, p.4117 ; 5219, 1980.
67. Arnold, G.S., Smith, I.W.M., Journ. Chem. Soc. Faraday Trans. II, (G.B.), vol.77, pt.6, p.861, 1981.
68. Krieger, K., Acta Phys. Poland A. vol. A61, p.571, 1982.
69. Magnitskii, S.A., Tunkin, V.G., Sov. Journ. Quant. Electr., vol. 11, p.1218, 1981.
70. Baumgarnter, R., Byer, R.L., Proc. of Soc. Photo-Opt. Instr. Engin. vol. 122, p.88, 1977.
71. Endemann, M., Byer, R.L. Opt. Letts. vol. 5, p.452, 1980.
72. Byer, R.L., Endemann, M., AIAAJ, vol. 20, p.395, 1982.
73. Wormhoudt, J., Steinfeld, J.I., Oppenheim, I., Journ. Chem. Phys. vol. 66, p.3121, 1977.
74. Wormhoudt, J., Marabella, L., Steinfeld, J.I., Sov. Journ. Quant. Electr. vol. 6, p.470, 1976.
75. Chu, T.B., Jurgeit, R., Nickles, P.V. Sov. Journ. Quant. Electr. vol. 7, p.1494, 1977.
76. Banin, A.A., Petryakov, V.N. Friedman, G.I., Sov. Journ. Electr. vol. 11, p.664, 1981.
77. Akhmanov, S.A., Kovrigin, A.I., Kuznetsov, V.I., Pershin, S.M. Kholoduykh, A.I., Sov. Journ. Quant. Electr. vol. 8. p.113, 1978.
78. Zhdanov, B.V., Zheludev, N.I., Kovrigin, A.I., Kuznetsov, V.I., Sov. Journ. Quant. Electr. vol. 9, p.202, 1979.
79. Mochizuki, K., Namihira, Y., Wakabayashi, H., Electron. Letts. (G.B.) vol. 17, p.646, 1981.
80. Akhmanov, S.A., Picosecond Phenomena, p.134, 1978.

Acknowledgements

This work was supported by research grants from the Army Research Office, N.A.S.A. and D.O.E. We want to acknowledge Mary Farley for preparing the manuscript.

Recent Developments in the Growth of Chalcopyrite Crystals for Nonlinear Infrared Applications

R. S. Feigelson and R. K. Route

Center for Materials Research, Stanford University
105 McCullough Building, Stanford, CA 94305

Abstract

Improvements in crystal growth technology have enabled us to grow 28 mm dia., 10 cm long crack- and twin-free boules of the chalcopyrite compounds $AgGaS_2$ and $AgGaSe_2$. While the crystals grow with optical defects (micron-size scattering centers), post-growth heat treatment procedures have been used to successfully eliminate them and produce material of near-theoretical transparency. High optical quality, oriented single crystals, 1 cm in cross-section and over 2 cm in length have been produced and are leading to new advances in IR frequency generation.

The optical and phase equilibrium studies that have led to this advance in materials technology are described, as well as some of the details in the crystal growth technology itself.

Introduction

Silver thiogallate ($AgGaS_2$) and silver selenogallate ($AgGaSe_2$) are among the $I\text{-}III\text{-}IV_2$ compounds that crystallize in the chalcopyrite structure. It was shown over ten years ago that these two materials had unique non-linear infrared optical properties.[1-5] Both are highly nonlinear and each is continuously phase matchable throughout its transparency range, 0.45-13μm and 0.73-17μm respectively. Free carrier absorption is negligible since both are semi-insulating. Although reports of their use in nonlinear optical applications have appeared in the literature throughout the past fifteen years,[6-14] their full potential has never been realized due to challenging problems in crystal growth and control of optical quality.

Background

The two compounds $AgGaS_2$ and $AgGaSe_2$ are reactive and somewhat volatile at their melting points of MP = 996°C and MP = 856°C respectively. Hence both must be grown in sealed quartz growth ampoules. Their chalcopyrite structure, space group 42m, is based upon the zinc blende structure of the III-V's but has lower symmetry due to alternate ordering in the cation sublattice. The unit cell is tetragonal, shown in Fig. 1, and mechanical and optical properties are different in directions parallel to and normal to the optic, or c-axis.

Initial crystal growth experiments on these two materials revealed a number of problem areas including: (1) crystal and ampoule cracking, (2) bands of inclusions, (3) compositional grading, (4) twins and (5) poor optical quality.[15-19] The crystals had a milky appearance due to a high density of micron size scattering centers.[5,15-17,19-22]

One of the most important discoveries that has led to the successful growth of these materials was that by Korczak and Staff[19] when they found that $AgGaS_2$ has anomolous thermal expansion behavior, and actually expands along the c-axis as it is cooled. Iseler[14] soon showed that this was true for $AgGaSe_2$ as well, Fig. 2. The second important discovery was in working out a heat treatment procedure effective at eliminating the scattering centers in as-grown crystals. This was shown first by Matthes, et al.[20] for the case of $AgGaS_2$ and by Route et al.[23] for the case of $AgGaSe_2$. Our current highly successful crystal growth technology is based on the early work in these two areas.

Crystal growth technology

Materials synthesis

Both $AgGaS_2$ and $AgGaSe_2$ melt congruently, and some details of the phase equilibria in both systems[24, 25] along the pseudobinary $Ag_2S\text{-}Ga_2S_3$ and $Ag_2Se\text{-}Ga_2Se_3$ joins are known. The compounds are typically made by reaction of high purity, 5-9's or better, starting materials in elemental form in a separate procedure. In our work we have studied compositions close to stoichiometric. Chemical reaction is carried out in evacuated and sealed fused quartz ampoules which are internally coated with carbon by pyrolysis of an organic vapor. Because the vapor pressure over elemental sulfur exceeds the rupture strength of fused quartz ampoules at well below reaction temperature, a two-temperature vapor transport procedure is used to react $AgGaS_2$, Fig. 3. Elemental Se has much lower vapor pressures,

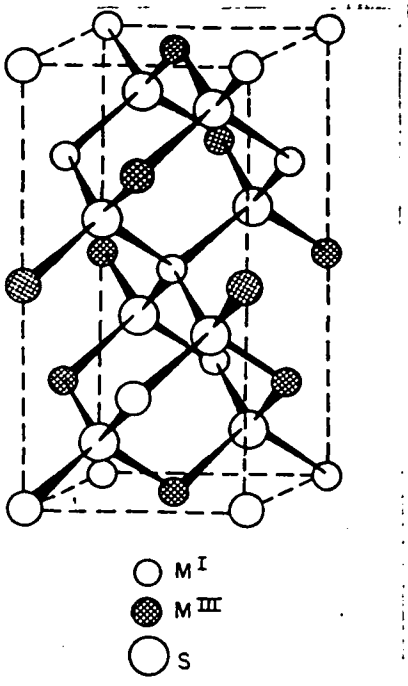

Figure 1. Unit cell of the chalcopyrite structure.

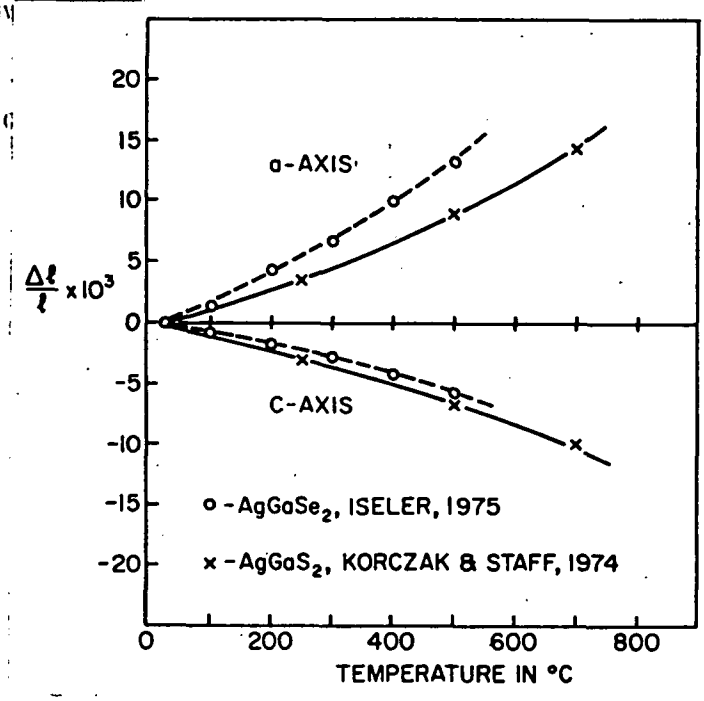

Figure 2. Thermal expansion properties showing properties having anomolous behavior along the optic, or c-axis.

and chemical reaction by direct fusion can be used for $AgGaSe_2$. In both cases, we harvest a polycrystalline charge which is highly cracked and shows evidence of compositional variations. (We now know this is unavoidable.) The material is then finely broken to achieve some degree of homogenization before it is used as a charge for crystal growth.

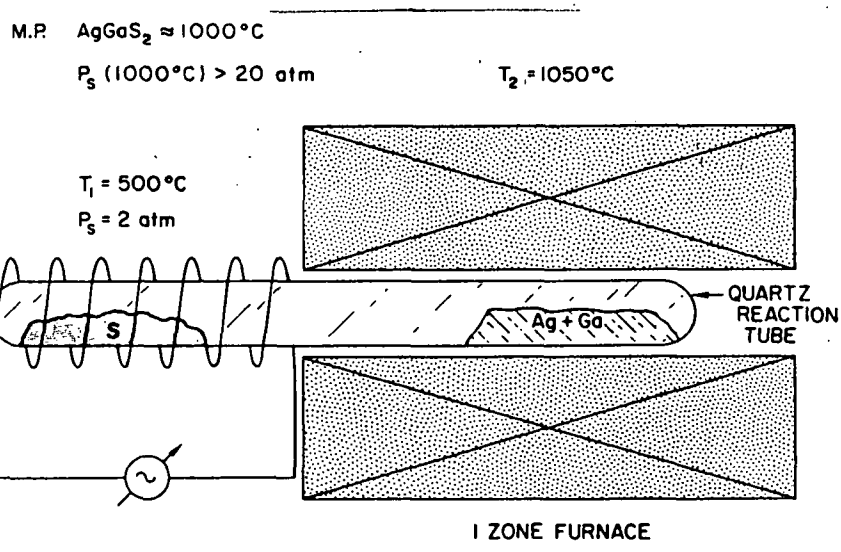

Figure 3. Vapor transport method for the synthesis of $AgGaS_2$ which prevents rupture of the quartz ampoule. When reaction is complete, the entire ampoule is raised to 1050° and agitated to achieve homogenization.

Crystal growth by the Bridgman method. Crystals are grown by the standard Bridgman-Stockbarger method in a 2-1/2" ID resistance wound tubular two-zone furnace. Temperature gradients at the growth interface were nominally 18°C/cm measured in the open bore. With the growth ampoule present this is reduced somewhat to ~14°C/cm. There are two essential features to the successful growth of $AgGaS_2$ and $AgGaSe_2$ in sealed quartz ampoules. First, since the crystals are known to expand along their optic [001] axis, during cooling, they must be seeded so that the c-axis is close to the axis of the growth ampoule. (Crystals which nucleate spontaneously typically end up with the c-axis tipped far enough over from

the ampoule axis that a net transverse expansion occurs during cooling, with disastrous results.) Second, since c-axis boules expand along their length during cooling, the ampoules must be designed so that mechanical restrictions along their lengths cannot occur. We have solved this problem by designing our fused quartz growth ampoules with a continuous 1-1/2° taper in both the seed pocket and the main body. The flare-out region is usually designed with a 20° internal half angle. Commercial fused quartz tubing cannot be selected and worked so as to introduce the appropriate taper while maintaining a perfectly round internal cross-section. To produce growth ampoules with the desired interior dimensions we have developed a vacuum-forming method by which slightly oversized fused quartz tubing can be collapsed upon a precision-machined graphite mandrel. Replication of the mandrel surface is exact and the internal finish is otherwise smooth except where machining imperfections on the mandrel surface have occurred. The growth ampoules used in this work were nominally 28 mm ID with a 6 mm dia. by 15 mm long seed pocket. A carbon mandrel and a vacuum-formed ampoule are shown in Fig. 4. Prior to use the growth ampoules were internally coated with carbon by pyrolysis of an organic vapor.

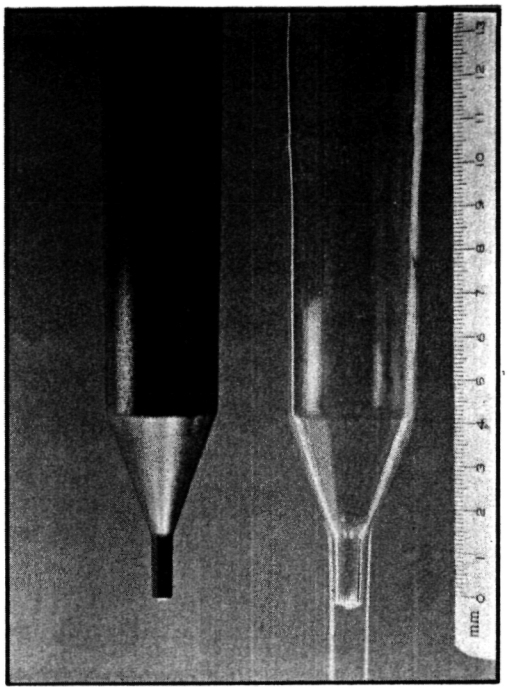

Figure 4. Precision tapered graphite mandrel and vacuum-formed fused quartz growth ampoule.

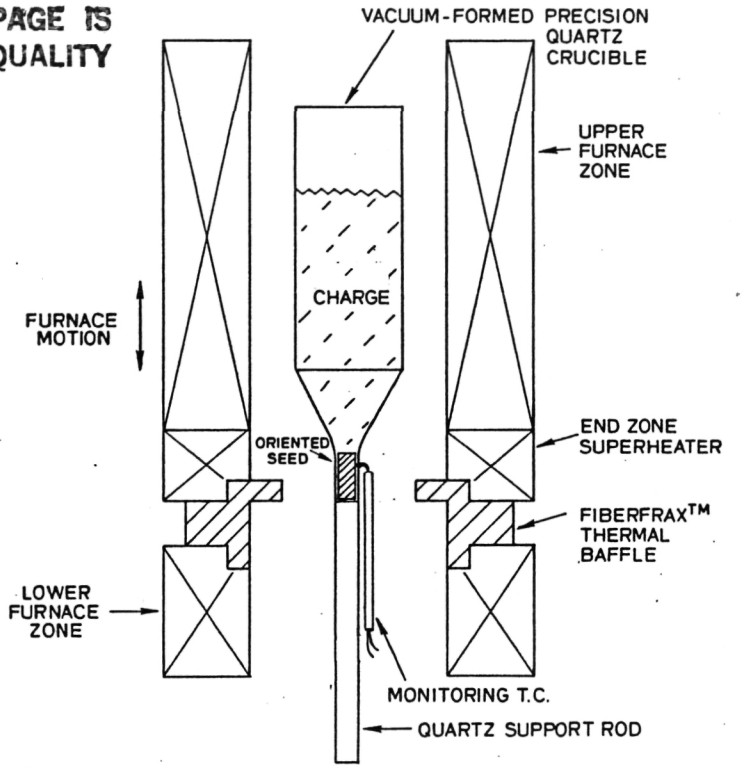

Figure 5. Bridgman furnace configuration showing thermocouple monitor by which meltback and seed attachment is controlled.

Accurately oriented c-axis seeds were hand-fitted to the growth ampoules by a taper grinding method. A few mils clearance was allowed for transverse thermal expansion during heat-up. Boules were designed to be 10-12 cm in length which required crushed polycrystalline charges of ~200 g. Prior to sealing, the charged growth ampoules were evacuated to pressures less than 10^{-5} Torr and were then back-filled with 0.5 atmosphere of argon gas purified by passing it through a titanium sponge reactor at 750°C. Seed attachment was controlled by monitoring a platinum-rhodium thermocouple held against the side of the seed pocket by spring tension, Fig. 5. Seeding temperatures were determined empirically, but were found to be quite close to the congruent melting points. Crystal growth was then carried out at approximately 15 mm/day. When solidification was complete, the crystals were cooled in the shallow gradient lower zone of the furnace at a rate of 50°C/hr.

Properly seeded boules were found to be loose in their ampoules after growth. Occasional secondary nucleation on the surfaces was observed and is thought to be related to failure of the carbon coating. Polycrystalline boules were always seriously cracked due to thermal expansion anisotropy. Minor surface spalling was also occasionally found around localized surface imperfections. In most cases, however, boules remained single and were of excellent structural quality. Refinement of our technique allowed us to grow crystals

with very few surface voids. Twins, present in almost all early work, did not occur as long as mechanical interaction with the growth ampoules was carefully prevented. Boules of $AgGaS_2$ and $AgGaSe_2$ free of structural imperfections are shown in Fig. 6. In both cases, compositional variations are observed independent of the charge composition. A thin band of black material, always found on the top of $AgGaS_2$ boules, was determined by dispersive analysis to be Ag- and S-rich and was assumed to be Ag_2S. When charges were made with ± 1% excess Ag_2S around the stoichiometric composition, Ag_2S was always rejected from the melts. Similar behavior was found for $AgGaSe_2$.

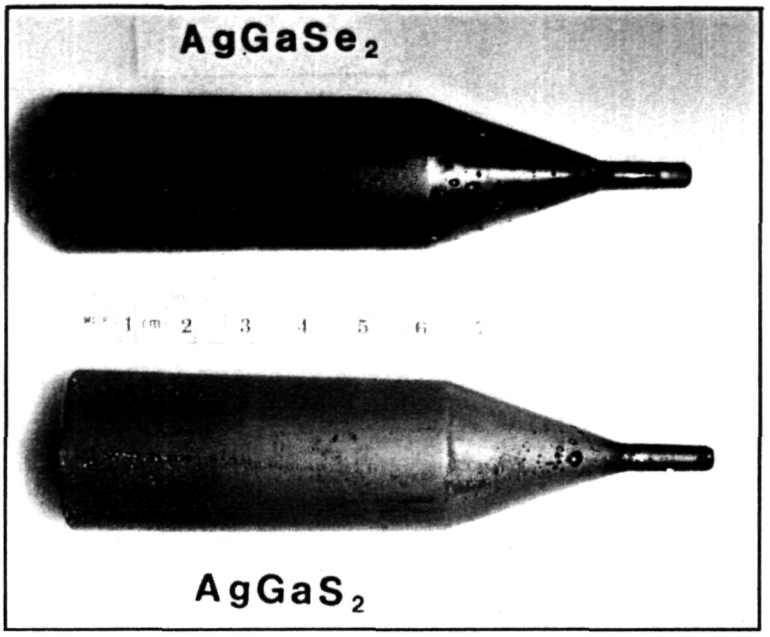

Figure 6. 28 mm twin- and crack-free boules of $AgGaSe_2$ and $AgGaS_2$.

Optical properties

Although structurally perfect, the as-grown crystals of both $AgGaS_2$ and $AgGaSe_2$ were always found to have a milky appearance. This can readily be seen in the case of $AgGaS_2$, Fig. 7 which is transparent at visible wavelengths. It can also be seen in $AgGaSe_2$ in thin section or with a commercial infrared image converter.

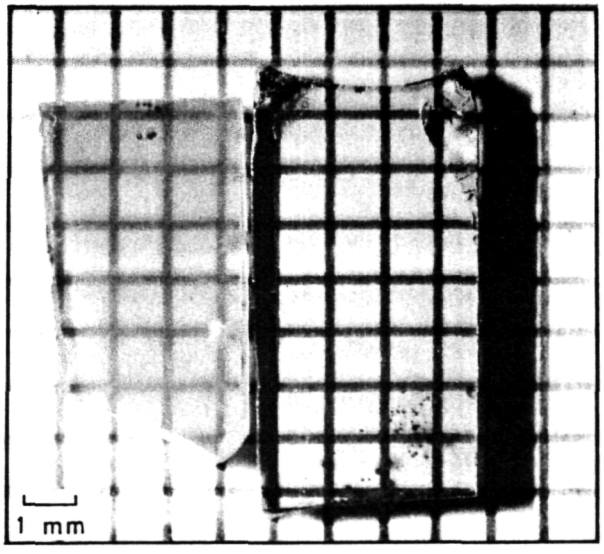

Figure 7. As-grown thin section of $AgGaS_2$ (left) showing milky appearance as compared to clear crystal (right).

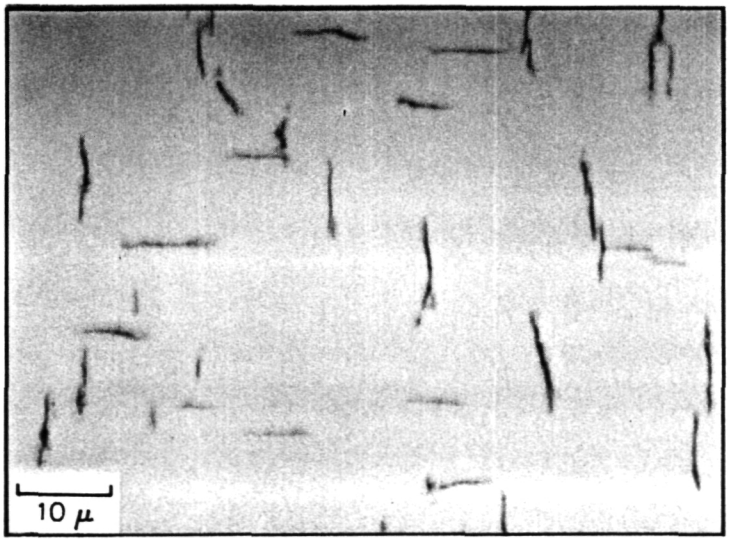

Figure 8. $AgGaS_2$ viewed along c-axis reveals microscopic scattering defects aligned along the [100] and [010] directions. Their lengths vary from 10-100 microns, and they appear to be microcracks.

Microscopic scattering centers. Microscopic examination of $AgGaS_2$ in transmitted light reveals micron-wide linear defects, ~100μm long oriented along the [100] and [010] directions, Fig. 8. Korczak and Staff[19] referred to them as microcracks which is exactly how they appear. More extensive metallographic preparation and optical microscopic evaluation was carried out in our laboratory, primarily on $AgGaS_2$. The defects were found to consist of precipitates surrounded by localized strain fields[26, 27], Fig. 9a. Careful etching and ion beam milling studies showed that the precipitates are actually 100 micron rectangular platelets lying on the (100) and (010) planes, Fig. 9b. The defects are slightly richer than the matrix in both Ga and S. A corresponding situation is true for the case of $AgGaSe_2$.

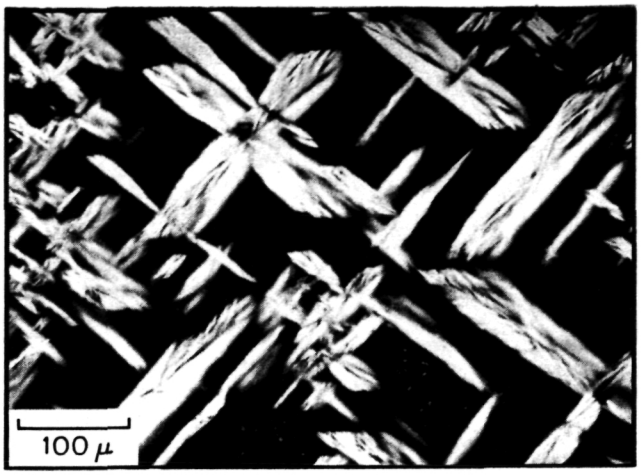

Figure 9a. Microscopic scattering defects and associated strain fields viewed in thin sections tilted off the basal plane somewhat. A blade-like shape at the core is suggested.

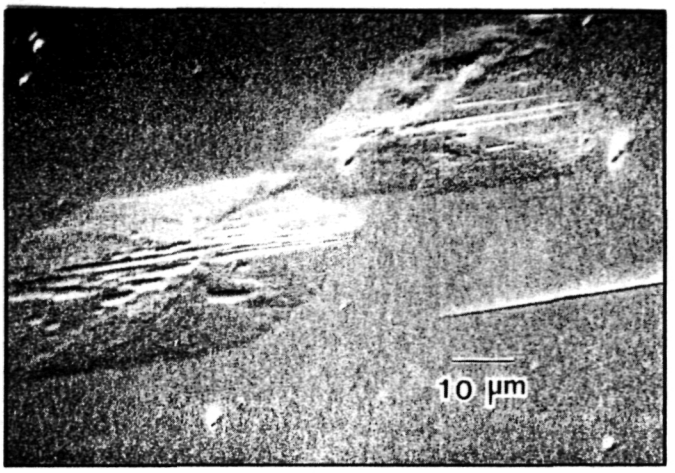

Figure 9b. Scattering defects are shown to be platelets with a rod-like fine structure lying in the (100) and (010) planes, as revealed by careful polishing and ion-beam milling.

Phase equilibrium studies. The precipitates and their surrounding strain fields can be removed from $AgGaS_2$ either by quenching from temperatures above 750°C, or by heat treatment at 900°C in the presence of Ag_2S.[20,23] DTA studies on compositions along the Ag_2S-Ga_2S_3 pseudobinary join in the vicinity of the stoichiometric composition were carried out here[28] and elsewhere[24] to ellucidate the detailed nature of the pseudobinary phase diagram. The DTA technique is quite sensitive. A problem occurs, however, in preparing test samples of precisely determined composition. In-situ synthesis is very difficult because of excessive pressures over any unreacted sulfur, and working from the binary end members is not reliable because Ga_2S_3 exists over a range of compositions. The maximum melting composition has been shown to lie ~ 1 mole % to the Ga_2S_3-rich side of stoichiometry [24]. The resolution of these studies was not adequate to reveal additional features at elevated temperatures. An existence region of finite width can be inferred from our earlier quenching studies, however, since the compound obviously lies in a single phase region at temperatures above 750°C. We therefore conclude that the original phase diagram of Brandt and Krämer,[24] Fig. 10a, should be modified to include an existence region of ~ 1 mole % width lying entirely on the Ga_2S_3-side of stoichiometry, Fig 10b. All crystals grown from near-stoichiometric melts thus contain excess Ga_2S_3 which precipitates as the crystals are cooled as an intermediate phase (presumably $Ag_2Ga_{20}S_{31}$) due to retrograde solubility . This model is consistent with our electron microprobe studies of precipitates in $AgGaS_2$, as well as the tendency of all $AgGaS_2$ boules to reject Ag_2S as they grow from stoichiometric melts.

The above model suggests that optically clear material, free of precipitates, might be grown from Ag_2S-rich solutions in which the liquidus temperature is below the point where the existence region departs from stoichiometry. A series of growth experiments was carried out from Ag_2S-rich solutions, as shown in Fig. 11, to demonstrate this effect. For solutions of greater than 65% Ag_2S, where the liquidus temperature is in the neighborhood of 960°C, optically clear crystals were obtained. The method is totally impractical for the controlled growth of large high quality crystals, however, due to the obvious difficulties in seeding and the need to reject large amounts of material from the growing crystal interface. The growth of high quality but cloudy crystals from congruent melts, followed by a heat treatment procedure turns out to be a far more effective approach.

A totally analogous situation exists for the case of $AgGaSe_2$, and in fact some evidence of a finite width existence region was found by Mikkelsen[25] in his phase equilibrium studies in the Ag_2Se-Ga_2Se_3 system.

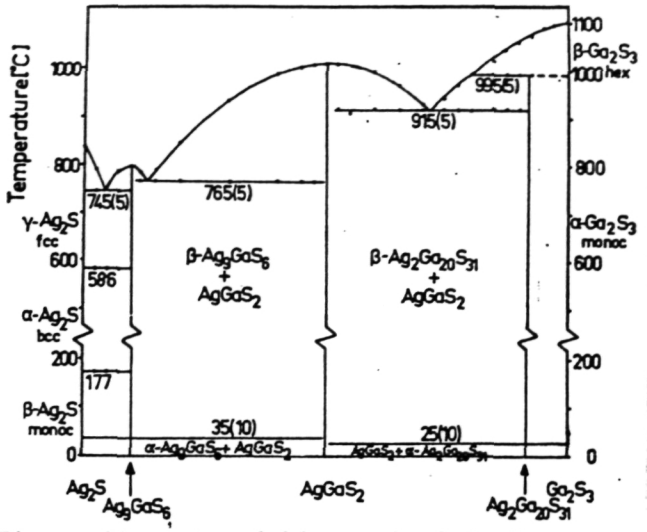

Figure 10a. Pseudobinary Ag_2S-Ga_2S_3 phase diagram of Brandt and Krämer [24].

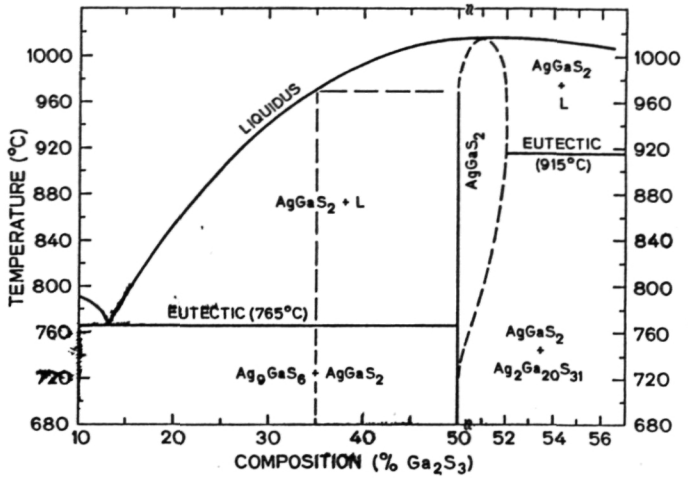

Figure 10b. Modified phase equilibria due to this work which suggests a 2% wide existence region lying entirely in the Ga_2S_3-rich side of stoichiometry.

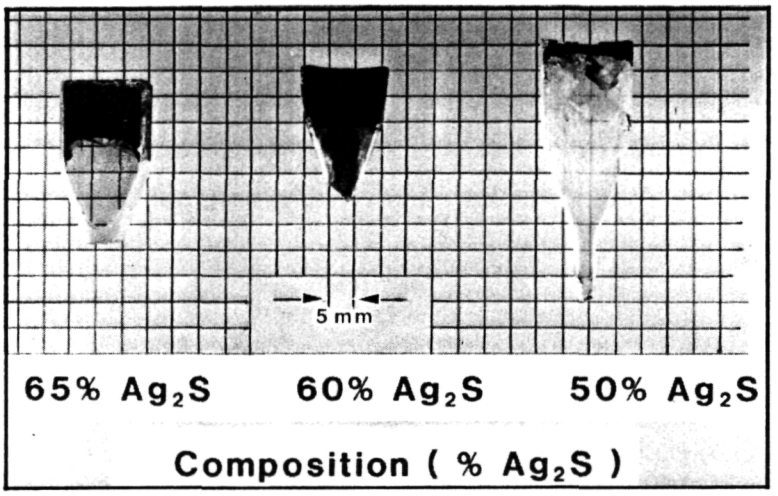

Figure 11. Growth of $AgGaS_2$ crystals from solutions rich in Ag_2S. $AgGaS_2$ free of scattering defects was obtained from a solution of composition 65m% Ag_2S - 35m% Ga_2S_3.

Heat treatment procedures. For the case of $AgGaS_2$, oriented slabs are first cut from as-grown boules. These are then heat treated in a sealed quartz ampoule for 10-15 days at 900°C according to the procedure shown in Fig. 12 and using approximately 0.5 wt % excess Ag_2S. During this period, Ga_2S_3 or $(2Ga + \frac{3}{2}S_2)$ apparently volatilizes from the surfaces of the crystals and reacts with the excess Ag_2S to form $AgGaS_2$ + L. Probably Ag and S diffusion cause the bulk crystal to homogenize to a composition on the left-hand boundary of the existence region, very near to stoichiometry and where retrograde solubility does not occur. Optically clear material results, as shown in Fig. 13. A similar process is used for $AgGaSe_2$.

On occasion defects that can not be removed by repeated heat treatment are found. These sometimes appear as negative crystals (internally faceted voids) and are thought to be caused by the incorporation of additional phases or the condensation of larger $Ag_2Ga_{20}S_{31}$ precipitates. Their presence, however, does not significantly affect optical transparency. In Fig. 14, we show transmission measurements made on as-grown, quenched, and heat-treated $AgGaS_2$ crystals. Careful heat treatment results in near-theoretical transparency throughout the entire transparency range. $AgGaS_2$ is useful for nonlinear frequency generation in the 0.5-10 μm wavelength range. An intrinsic multi-phonon absorption of 0.6 cm^{-1} near 10μm[29], however, limits its use for second harmonic generation of the

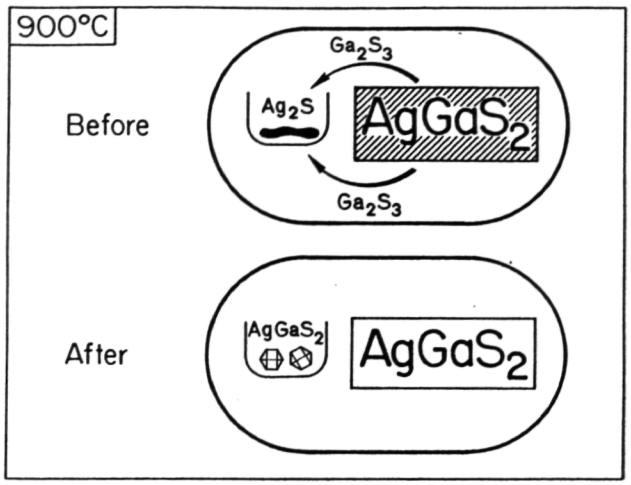

Figure 12. Post-growth heat treatment method used to eliminate optical scattering defects from $AgGaS_2$ crystals.

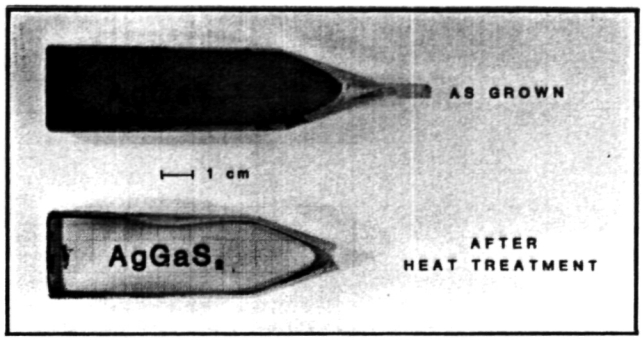

Figure 13. Comparison of heat-treated vs. as-grown boules (11 mm thick).

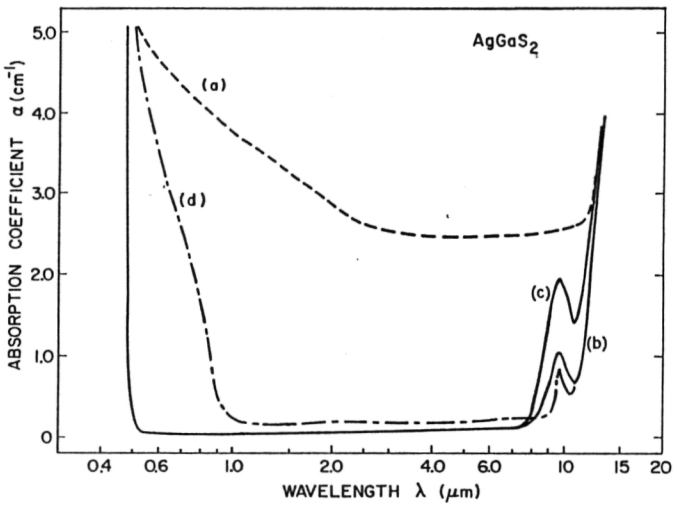

Figure 14. Spectral absorption of $AgGaS_2$ (a) as-grown; (b) quenched from 900°C; (c) heat-treated with Ag_2S, (d) heat-treated with Ag_2S and then with S.

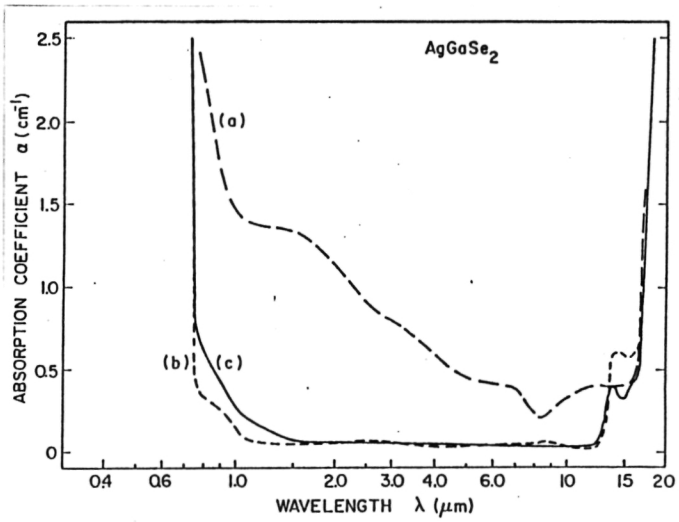

Figure 15. Spectral absorption of $AgGaSe_2$ (a) as-grown, (b) quenched from 650°C, (c) heat-treated with Ag_2Se.

10.6μm line from the CO_2 laser. The restrahlen bands in $AgGaSe_2$ are located at much longer wavelengths, and this material is well-suited to the application. It, too, is produced as a near-theoretically transparency crystal by an analogous heat treatment procedure, Fig. 15.

Optical crystals

Using the crystal growth and post-growth heat treatment procedures described, we have been successful in producing near theroetically transparent oriented crystals approximately 1 cm in cross-section. The lengths vary slightly depending on the propagation direction which is determined by the phase matching conditions. For most experiments we have been able to fabricate crystals in excess of 22 mm long from our nominal 28 mm dia. boules, Fig. 16. Most crystals end up being cut between 45°-90° to the boule axis. For all useful phasematching conditions, we are prevented from growing the crystals sufficiently close to the propagation direction to harvest substantially larger crystals, because of the anomolous thermal expansion problem. Hence, to obtain longer interaction lengths, crystals of larger diameter appear to be required.

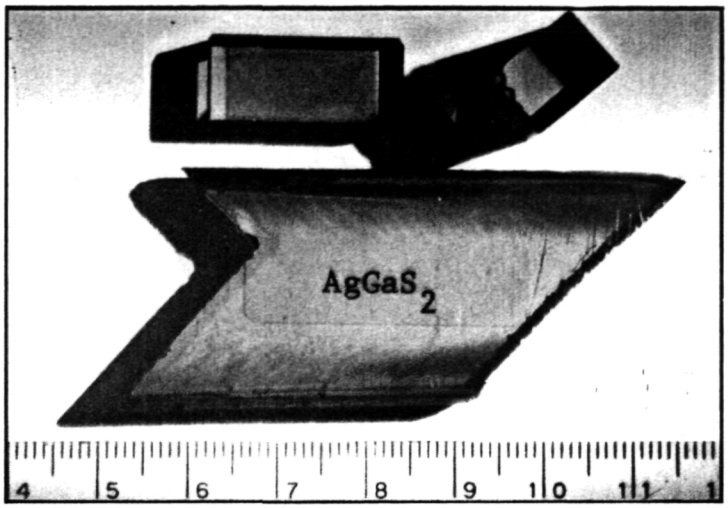

Figure 16. Fabricated crystals of $AgGaS_2$.

Recent non-linear optical results

With high optical quality twin-free crystals of both $AgGaS_2$ and $AgGaSe_2$ now available, significant advances in nonlinear IR optical technology are being made. Principal among these are the demonstration of optical parametric oscillation in $AgGaS_2$[30] and efficient second harmonic conversion of the carbon dioxide laser[31]. Details of these experiments are included in Table I.

The limitation of both materials is now due to their relatively moderate threshold for surface damage, which is in the 10-15 MW/cm^2 range. Preliminary experimentation with various anti-reflection surface coatings indicate that these values may be raised by a factor of two or more and consequently, higher conversion efficiencies should be possible. The alternative approach is, of course, to grow larger boules from which longer (and hence more efficient) crystals can be obtained.

Table 1. Results of nonlinear experiments on $AgGaS_2$ and $AgGaSe_2$

Experiment	Results	Reference
Infrared parametric oscillation in $AgGaS_2$	pump wavelength: 1.06 μm output wavelength: tunable from 1.4 to 4.0 μm threshold: 1.2 mJ peak energy conversion: 16%	30
Second harmonic generation in $AgGaSe_2$	pump wavelength: 10.25 μm output wavelength: 5.13 μm energy conversion efficiency: 14%	31
Infrared parametric oscillation in $AgGaSe_2$	pump wavelength: 1.338 μm output wavelengths: narrowly tunable around 1.6 and 7 μm. (This was a preliminary measurement demonstrating parametric oscillation. Widely tunable output between 2.4 and 12.5 μm would be possible with a 2.0 μm pump source.)	32
Damage threshold measurements for $AgGaS_2$ and $AgGaSe_2$	Surface damage threshold were measured at both 1.06 μm and 10.6 μm. Typical values for damage threshold are near 13 MW/cm^2. Some anti-reflection coatings almost doubled the threshold for surface damage.	30, 31, 32

Conclusions

The practical problems associated with the growth of high optical quality, twin-free crystals of both $AgGaS_2$ and $AgGaSe_2$ have been resolved. Near theoretically transparent crystals in excess of 2 cm long by 1 cm in cross-section have been produced from 28 mm boules. With these, useful and practical solid-state nonlinear infrared optical devices are now being realized.

Acknowledgement

This work was supported by the NSF/MRL Program through the Center for Materials Research at Stanford University, the U. S. Army Research Office, NASA, SRI International, and Quanta-Ray, Inc.

References

1. D. S. Chemla, P. J. Kupecek, D. S. Robertson and R. C. Smith, Opt. Commun. 3, 29 (1971).
2. G. D. Boyd, H. Kasper and J. H. McFee, IEEE J. Quantum Electron. QE-7, 563 (1971).
3. G. D. Boyd, H. M. Kasper, J. H. McFee, and F. G. Storz, IEEE J. Quantum Electron. QE-8, 900 (1972).
4. H. Kildal and J. C. Mikkelsen, Opt. Commun. 9, 315 (1973).
5. G. C. Bhar and R. C. Smith, Phys. Stat. Solidi A-13, 157 (1972).
6. W. Jantz and P. Koidl, Appl. Phys. Lett. 31, 99 (1977).
7. T. Elsaesser, A. Seilmeier, and W. Kaiser, Appl. Phys. Lett. 44, 383 (1984).
8. R. L. Byer, M. M. Choy, R. L. Herbst, D. S. Chemla, and R. S. Feigelson, Appl. Phys. Lett., 24, 65 (1974).
9. R. J. Seymour and F. Zernike, Appl. Phys. Lett., 29, 705 (1976).
10. D. C. Hanna, V. V. Rampal, and R. C. Smith, Opt. Commun. 8, 151 (1973).
11. D. Fröhlich, K. Reimann, and P. Koidl, Phys. Stat. Solidi B-114, 553 (1982).
12. K. Kato, IEEE J. Quantum Electron. QE-20, 698 (1984).
13. H. Kildal and J. C. Mikkelsen, Opt. Commun. 9, 315 (1973).
14. G. W. Iseler, J. Crystal Growth 41, 146 (1977).
15. H. A. Chedzey, D. J. Marshall, H. T. Parfitt and D. S. Robertson, J. Phys. D4, 1320 (1971).
16. B. Tell and H. M. Kasper, Phys. Rev. B4, 4455 (1971).
17. H. M. Kasper, Nat. Bur. Std. (US) Special Publ. 364, 671 (1972).
18. P. W. Yu and Y. S. Park, J. Appl. Phys. 45, 823 (1974).
19. P. Korczak and C. B. Staff, J. Crystal Growth 24/25, 386 (1974).
20. H. Matthes, R. Viehmann and N. Marschall, Appl. Phys. Lett. 26, 237 (1975).
21. R. K. Route, R. J. Raymakers and R. S. Feigelson, J. Crystal Growth 24/25, 390 (1974).
22. R. K. Route, R. J. Raymakers and R. S. Feigelson, J. Crystal Growth 29, 125 (1975).
23. R. K. Route, R. S. Feigelson, and R. J. Raymakers, J. Crystal Growth 33, 239 (1976).
24. G. Brandt and V. Krämer, Mat. Res. Bull. 11, 1381 (1976).
25. J. C. Mikkelsen, Jr., Mat. Res. Bull. 12, 497 (1977).
26. R. Koch, R. K. Route and R. S. Feigelson, Il Nuevo Cimento 2D, 1767 (1982).
27. R. S. Feigelson, R. Koch, R. K. Route and C.-E. Huang, Collected abstracts, VII International Conference on Crystal Growth, Stuttgart, Germany, FR (1983).
28. Unpublished work.
29. G. C. Bhar and R. C. Smith, IEEE J. Quantum Electron. QE-10, 546 (1974).
30. Y.-X. Fan, R. C. Eckardt, R. L. Byer, R. K. Route and R. S. Feigelson, Appl. Phys. Lett. 45, 313 (1984).
31. R. C. Eckardt, Y.-X. Fan, R. L. Byer, R. K. Route, R. S. Feigelson, and J. van der Laan, "Efficient Second Harmonic Generation of 10 Microns in $AgGaSe_2$," presented at CLEO, Baltimore, May 1985; to be published.
32. R. C. Eckardt, Y.-X. Fan, R. L. Byer; to be published.